

# BAXTER TREE-LIKE TABLEAUX

ABSTRACT. Tree-like tableaux are objects in bijection with alternative or permutation tableaux. They have been the subject of a fruitful combinatorial study for the past few years. In the present work, we define and study a new subclass of tree-like tableaux enumerated by Baxter numbers. We exhibit simple bijective links between these objects and three other combinatorial classes: (packed or mosaic) floorplans, twisted Baxter permutations and triples of non-intersecting lattice paths. From several (and unrelated) works, these last objects are already known to be enumerated by Baxter numbers, and our main contribution is to provide a unifying approach to bijections between Baxter objects, where Baxter tree-like tableaux play the key role. We moreover get new enumerative results about alternating twisted Baxter permutations. Finally, we define a new subfamily of floorplans, which we call alternating floorplans, and we enumerate these combinatorial objects.

Keywords: Tree-like tableau; Baxter number; floorplan; twisted Baxter permutation; non-intersecting lattice path.

## 1. INTRODUCTION

Baxter permutations are named after the mathematician Glen<sup>1</sup> Baxter [5], who introduced them in 1964 (in an analysis context). They are enumerated by *Baxter numbers* [25, sequence A001181], whose formula was obtained by Chung *et al.* [10] (see also [26] for a combinatorial proof):

$$Bax_n = \frac{2}{n(n+1)^2} \sum_{k=1}^n \binom{n+1}{k-1} \binom{n+1}{k} \binom{n+1}{k+1}.$$

Since then, Baxter numbers have appeared to enumerate various classes of combinatorial objects: pairs of twin binary trees [13], several kinds of standard Young tableaux with three rows [14, 9], plane bipolar orientations [6, 7], and three other classes that we shall present in more details, as they play important parts in our work.

The first one is the class of *twisted Baxter permutations*. These permutations were defined a few years ago by Reading in an algebraic context [23]: they naturally index bases for subalgebras of the Malvenuto-Reutenauer Hopf algebra of permutations. Like Baxter permutations, twisted Baxter permutations may be characterized by pattern avoidance, and West proved [29] (by a recursive bijection) that they are enumerated by Baxter numbers. These objects are also endowed with a nice Hopf structure, as revealed by the recent works [20, 17].

---

*Date:* March 19, 2021.

*Key words and phrases.* combinatorial graph theory, combinatorial probability, cographs, random graphs, graphons, self-similarity.

<sup>1</sup>Not to be confused with the physicist Rodney Baxter.

The second class we are interested in is a class of *triples of non-intersecting lattice paths*. The Lindström-Gessel-Viennot lemma [21, 16] relates the enumeration of non-intersecting lattice paths (NILP) to the computation of determinants of integer matrices. Because of that, NILPs are ubiquitous objects that appear in many contexts in combinatorics. The class we shall consider here is known [14] to be in bijection with pairs of twin binary trees, see their precise definition in Section 5.

The third and last class we shall present here is the class of *mosaic floorplans*. The notion of floorplans finds its origin in integrated circuits: a floorplan encodes the relative positions of modules in a circuit. A mosaic floorplan may be defined as an equivalence class of some rectangular partitions of a rectangle (called floorplans). They were proved to be enumerated by Baxter numbers [24], and a bijection was found with pairs of twin binary trees [30]. We introduce here combinatorial objects that we call *packed floorplans*: they are canonical representatives of mosaic floorplans, in the sense that every mosaic floorplan contains exactly one packed floorplan.

The goal of the present work is to link together these three combinatorial classes through the use of new objects that we call *Baxter tree-like tableaux*. Tree-like tableaux (TLTs) are combinatorial objects introduced in [3] as a new presentation of alternative or permutation tableaux [22, 27], and have revealed interesting combinatorial properties [3, 4]. Baxter TLTs are defined in a very simple way by avoidance of *patterns* (a notion to be defined in Section 2) in TLTs. We mention here that Felsner *et.al.* also provide bijective links between combinatorial structures enumerated by Baxter numbers in their paper [15]. But whereas their work is focused on twin binary trees and leads to Baxter permutations, the central objects of this present article are Baxter TLTs and our bijections lead to twisted Baxter permutations.

The outline of the paper is as follows. Section 2 introduces our new class of Baxter tree-like tableaux. Moreover, we recall in this section the recursive structure of tree-like tableaux, which has already proved to be the key tool dealing with these objects, and will be essential for the work reported here. Next, Sections 3, 4 and 5 are respectively devoted to packed floorplans, twisted Baxter permutations and triples of non-intersecting lattice paths: we define these three combinatorial classes and in each case, we build a simple bijection with Baxter TLTs. In Section 6, we consider the restriction of our construction to *alternating* objects. This allows us to obtain new combinatorial results, such as the enumeration of alternating twisted Baxter permutations (see Corollary 48), and to identify several enumerative questions which remain open.

## 2. BAXTER TREE-LIKE TABLEAUX

**2.1. Tree-like tableaux: definitions and useful tools.** We refer to [3] for a detailed study of tree-like tableaux. Here, we shall only recall the main definition and a few important properties.

**Definition 1** (Tree-like tableau). *A tree-like tableau (TLT) is a Ferrers diagram (drawn in the English notation) where each cell is either empty or pointed (i.e., occupied by a point), with the following conditions:*

- (1) the top leftmost cell of the diagram is occupied by a point, called the root point;
- (2) for every non-root pointed cell  $c$ , there exists a pointed cell  $p$  either above  $c$  in the same column, or to its left in the same row, but not both;  $p$  is called the parent of  $c$  in the TLT;
- (3) every column and every row contains at least one pointed cell.

The size of a TLT is the number of pointed cells it contains.

These objects were named tree-like tableaux because of the underlying tree structure they contain: recording the parent relations between the points of a TLT indeed produces a tree, whose root is the root point of the TLT. In this tree, every internal (*i.e.*, non-leaf) vertex may have either a right child (shown by a horizontal edge), or a left child (shown by a vertical edge), or both. We refer to such trees as *binary trees* (although they would more appropriately be called *incomplete binary trees*). Figure 1 (left) shows an example of TLT, with its underlying binary tree. The reader interested in more details about the underlying trees of TLTs may find them in [4, 3].

**Definition 2.** A ribbon in a TLT  $T$  is a set  $R$  of cells along the Southeast border of  $T$ , that is connected (with respect to edge-adjacency), does not contain any  $2 \times 2$  square, and consists only of non-pointed cells. Moreover it is required that the bottom leftmost cell of  $R$  is to the right of a pointed cell with no cell of  $T$  below it, and that the top rightmost cell of  $R$  is below a pointed cell.

Figure 1 (right) shows an example of a TLT of size 20 with a ribbon indicated by shaded cells (of magenta color).

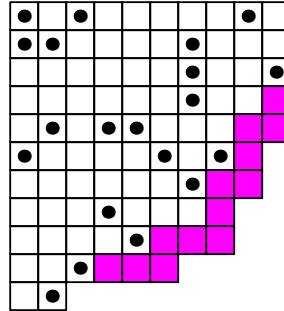


FIGURE A FAIRE

FIGURE 1. Left: A tree-like tableau  $T$  of size 20, with its underlying binary tree. Right: The same tree-like tableau  $T$  with a ribbon in  $T$ .

In the article [3] that defines TLTs, the so-called *insertion procedure*  $InsertPoint$  is defined. It allows to generate all TLTs unambiguously from the unique TLT of size 1  $\blacksquare$  by insertion of points (together with a row or column, and possibly a ribbon, of empty cells) at the *boundary edges* of TLTs, that is to say at edges of their Southeast border. We refer to [3] for details about this insertion procedure, and for proofs of statements about it in the remainder of this subsection.

This insertion procedure can also be interpreted as representing a *generating tree* of TLTs. A *generating tree* (see [28]) for a combinatorial class  $\mathcal{C}$  is simply an infinite rooted tree, whose vertices are the objects of  $\mathcal{C}$ , each appearing exactly once in the tree, and such that objects of size  $n$  are at distance  $n - 1$  from the root. An obvious remark that will be useful for us is the following: if  $\mathcal{C}$  and  $\mathcal{C}'$  admit generating trees which are isomorphic, then they are in size-preserving bijection. In terms of generating trees, the main result (Theorem 2.3) of [3] can be interpreted as follows: the infinite tree with root  $\blacksquare$ , where all children of a given TLT  $T$  are the TLTs obtained applying *InsertPoint* on  $T$  at each of the boundary edges of  $T$ , is a generating tree for TLTs.

The insertion procedure on TLTs also induces a canonical labeling of the  $n$  points of a TLT  $T$  of size  $n$  by the integers in  $\{1, \dots, n\}$ . It indicates the (unique) order in which the points of  $T$  have been inserted to obtain  $T$  from the empty TLT. This labeling is essential for the bijections that we define in Sections 3 and 4, and we review it now. Actually, this labeling may alternatively be described as the order in which the points of  $T$  should be *removed* with the procedure *RemovePoint* of [3] to go from  $T$  to  $\blacksquare$  (the unique TLT of size 1), and this is how we define it here. This is illustrated on Figure 2.

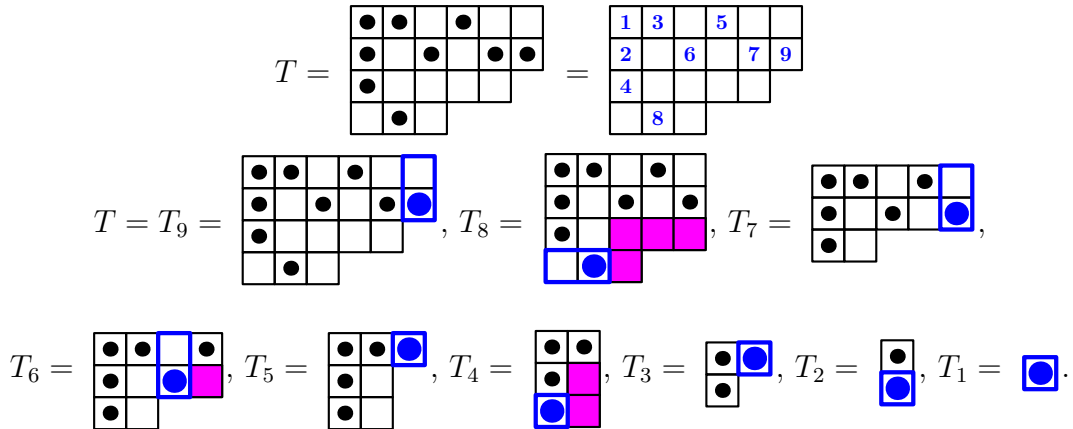


FIGURE 2. The labeling of the points of a TLT using the procedure *RemovePoint* recursively. The special points together with the associated columns (resp. rows) are denoted in boldface (of blue color), whereas the ribbons are indicated by shaded cells (of magenta color).

Consider a TLT  $T$  of size  $n$ . We define the *special point*  $s$  of  $T$  as: the point at the bottom of its column, which is Northeastmost among such points. (Notice that  $s$  always exists, since the bottom row of  $T$  contains at least one point, by definition.) This special point  $s$  gets the label  $n$ . To label the remaining  $n - 1$  points of  $T$ , we compute from  $T$  and  $s$  another TLT  $T'$  of size  $n - 1$ , by removing  $s$  and some empty cells in  $T$ . The points of  $T'$  are in immediate correspondence with those of  $T$  except  $s$ , so that we may label in  $T$  the special point of  $T'$  with  $n - 1$ , and proceed recursively. We will denote by

$(T_n = T, T_{n-1} = T', T_{n-2}, \dots, T_1 = \blacksquare)$  the corresponding sequence of TLTs (each  $T_i$  having size  $i$ ).

We now explain how to build  $T'$  from  $T$  and  $s$ . Unless  $n = 1$ ,  $s$  is not the root point of  $T$ , and this implies that exactly one of the followings holds: either there is no point of  $T$  above  $s$  in the same column, or there is no point of  $T$  to its left in the same row. In the former (resp. latter) case, we define the *column* (resp. *row*) of  $s$  to be the cells above (resp. to the left of)  $s$  in the same column (resp. row). If there is a cell adjacent to  $s$  on its right, then this cell is empty (by definition of  $s$ ). In this case, we claim that there is a ribbon in  $T$  to the right of  $s$ . Indeed, this is derived from the two following facts: starting from the empty cell to the right of  $s$ , and following the Southeast border of  $T$ , we eventually meet a pointed cell  $p$ , since the last column of  $T$  contains a point; and  $p$  has been reached from below, since otherwise  $s$  would not be the special point. We call this set of empty cells the *ribbon of  $s$* . Now,  $T'$  is obtained from  $T$  by removing  $s$ , together with its column (resp. row) and its ribbon (when it exists).

From now on, when we speak of the ribbons of  $T$ , we mean the ribbons removed when applying iteratively the procedure *RemovePoint* from  $T$  until  $\blacksquare$  is reached.

**Observation 3.** *For a TLT  $T$  and two pointed cells  $c$  and  $c'$  with respective labels  $i$  and  $j$ . The following assertions are equivalent:*

- (1)  $c$  is (strictly) to the left and below  $c'$  and  $i = j + 1$ ;
- (2) there is a ribbon of  $T$  between  $c$  and  $c'$ .

To conclude the general properties of TLTs, we observe a property of the cells of its ribbons.

**Definition 4.** *A crossing in a TLT  $T$  is an empty (i.e., non-pointed) cell such that there are pointed cells both above it in the same column and to its left in the same row.*

This terminology has already been introduced in [3]. The choice of the word *crossing* is explained because such cells are those where two edges of the underlying binary tree of  $T$  cross each other.

will be used mostly in Sections 3 and 4, but also on a few occasions before.

**Definition 5.** *Let  $T$  be a TLT of size  $n$ , and denote by  $(T_n = T, T_{n-1}, T_{n-2}, \dots, T_1 = \blacksquare)$  the sequence of TLTs (each  $T_i$  having size  $i$ ) obtained iterating the procedure *RemovePoint* starting from  $T$ . For any cell  $c$  of the ribbon removed from  $T_i$  to obtain  $T_{i-1}$ , we define the label  $\text{rib}(c) = i$ .*

This labeling is illustrated on Figure 3. It will be used in Lemma 27.

Notice that there are cells with no rib-label. Indeed, we have the following characterization of cells having a rib-label:

**Observation 6.** *A cell has an rib-label if and only if it is a crossing.*

*Proof.* Note that TLTs have no empty rows nor columns. Therefore the definition of ribbons ensures that if a cell has a rib-label then it is a crossing. Conversely, considering a crossing  $c$  and the smallest  $i$  such that the cell  $c$  belongs to  $T_i$ , we obtain that  $c$  belongs to the ribbon removed from  $T_i$  to obtain  $T_{i-1}$ , hence has an rib-label (equal to  $i$ ).  $\square$

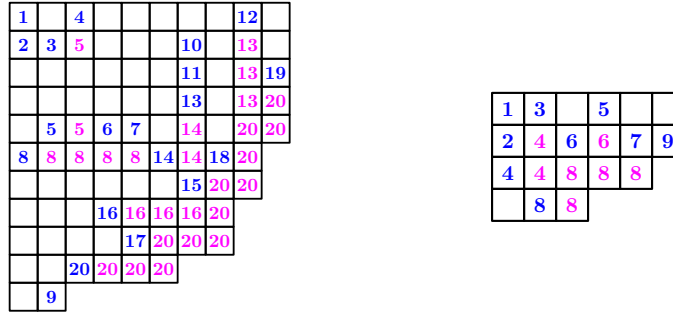


FIGURE 3. The labeling (of blue color) and the rib-label (of magenta color) of the TLTs of Figures 1 (left) and 2 (right).

**2.2. A family of TLTs enumerated by Baxter numbers.** In this work, we are interested in a family of TLTs restricted by pattern avoidance constraints. A TLT  $T$  is said to contain the pattern  $\begin{smallmatrix} \bullet & \bullet & \bullet \\ \bullet & \bullet & \bullet \end{smallmatrix}$  if there exist 2 rows and 3 columns in  $T$  such that the restriction of  $T$  to the  $2 \times 3 = 6$  cells at their intersection is equal to  $\begin{smallmatrix} \bullet & \bullet & \bullet \\ \bullet & \bullet & \bullet \end{smallmatrix}$  or  $\begin{smallmatrix} \bullet & \bullet & \bullet \\ \bullet & \bullet & \bullet \end{smallmatrix}$ . We define in the same way the pattern  $\begin{smallmatrix} \bullet & \bullet \\ \bullet & \bullet \end{smallmatrix}$ . With this kind of notation, the condition that every pointed cell in a TLT does not have pointed cells both above in the same column and to the left in the same row is expressed by the avoidance of the pattern  $\begin{smallmatrix} \bullet & \bullet \\ \bullet & \bullet \end{smallmatrix}$ .

**Definition 7** (Baxter tree-like tableau). *A Baxter tree-like tableau is a TLT which avoids (i.e., does not contain any of) the patterns  $\begin{smallmatrix} \bullet & \bullet & \bullet \\ \bullet & \bullet & \bullet \end{smallmatrix}$  and  $\begin{smallmatrix} \bullet & \bullet \\ \bullet & \bullet \end{smallmatrix}$ . We shall denote by  $\mathcal{T}_{(k,\ell)}$  the set of Baxter TLTs with  $k$  rows and  $\ell$  columns and set:  $\mathcal{T}_n = \sqcup_{k+\ell-1=n} \mathcal{T}_{(k,\ell)}$  where  $\sqcup$  denotes the disjoint union.*

We may remark that at each step of the procedure *RemovePoint*, one point is removed and either a row or a column is removed. This implies that the size of a TLT is given by its semi-perimeter-1. As a consequence, the size of any  $T \in \mathcal{T}_n$  is  $n$ . Figure 4 shows all Baxter TLTs  $(T^i)_{1 \leq i \leq 22}$  of size 4.

We may also note that the generating tree for TLTs induced by the procedure *InsertPoint*, can be restricted to Baxter TLTs, yielding a generating tree for Baxter TLTs. Indeed, the procedure *RemovePoint* applied to any Baxter TLT produces a Baxter TLT again (since applying *RemovePoint* cannot create any occurrence of  $\begin{smallmatrix} \bullet & \bullet & \bullet \\ \bullet & \bullet & \bullet \end{smallmatrix}$  or  $\begin{smallmatrix} \bullet & \bullet \\ \bullet & \bullet \end{smallmatrix}$ ).

Sections 3 to 5 describe size-preserving bijections between Baxter TLTs and families of objects that are known to be enumerated by *Baxter numbers*, hence their name. Specifically, Section 3 (resp. 4, resp. 5) describes a bijection denoted  $\Phi_{\mathcal{F}}$  (resp.  $\Phi_{\mathcal{B}}$ , resp.  $\Phi_{\mathcal{P}}$ ) between Baxter TLTs and (packed) floorplans (resp. inverses of twisted Baxter permutations, resp. triples of non-intersecting lattice paths). These bijections are illustrated in size 4 by Figures 7, 15 and 21 (p. 10, 22 and 28), where each TLT  $T^i$  of Figure 4 is sent to  $F^i$ ,  $\sigma^i$  and  $\pi^i$  by the bijections  $\Phi_{\mathcal{F}}$ ,  $\Phi_{\mathcal{B}}$  and  $\Phi_{\mathcal{P}}$ , respectively.

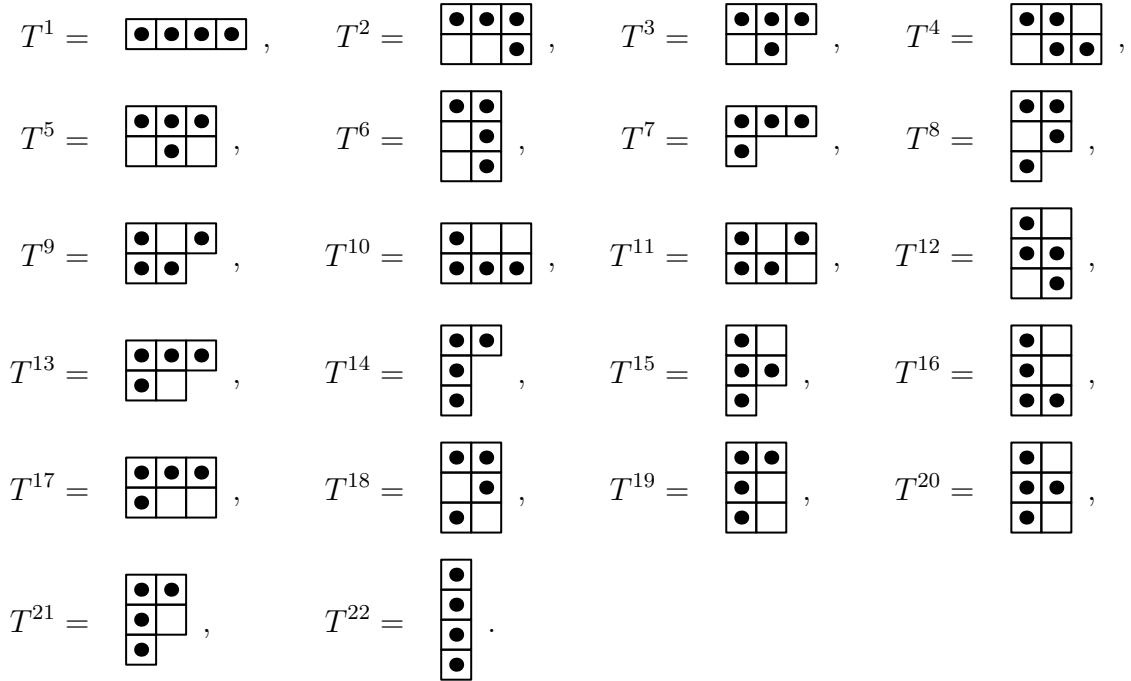


FIGURE 4. The 22 Baxter TLTs of size 4.

Before moving on to the announced bijections between Baxter TLTs and other Baxter objects, we make an observation that relates the tree structure of Baxter TLTs and the relative placement of their points.

**Proposition 8.** *Let  $T$  be a Baxter TLT. Consider the bi-partition  $(L, R)$  of the non-root points of  $T$ , where  $L$  (resp.  $R$ ) contains all points of  $T$  that are in the left (resp. right) subtree pending from the root of the underlying tree of  $T$ . Then all points of  $L$  are to the left and below all points of  $R$ .*

*Proof.* The proof is by contradiction. Assume that there is a point  $\ell \in L$  that lies to the right of a point  $r$  of  $R$ . Among all ancestors of  $r$  (including  $r$ ) in the underlying tree of  $T$ , there is one which lies to the left of  $\ell$  and above  $\ell$ . Indeed, all ancestors of  $r$  are to the left of  $r$ ,  $\ell$  does not lie in the first row of  $T$  (since it belongs to  $L$ ), and  $r$  has at least one non-root ancestor in the first row of  $T$  (since it belongs to  $R$ ). Denote  $r'$  such an ancestor of  $r$ . We have then that  $r'$  is above and to the left of  $\ell$ . Among all ancestors of  $\ell$  (including  $\ell$ ), denote by  $\ell'$  the one closest to the root of  $T$  such that  $r'$  is above and to the left of  $\ell'$ . This ensures that  $\ell'$  cannot be the root of  $T$ , and that together with the parent of  $\ell'$ ,  $\ell'$  and  $r'$  form a pattern  $\begin{bmatrix} \bullet & \bullet \\ \bullet & \bullet \end{bmatrix}$  or  $\begin{bmatrix} \bullet & \\ \bullet & \bullet \end{bmatrix}$ , a contradiction.

Assuming instead that there is a point  $\ell \in L$  that lies above of a point  $r$  of  $R$ , we derive a contradiction in a symmetric fashion.  $\square$

Several consequences of Proposition 8 will be useful in proving properties of our bijections.

**Corollary 9.** *Any binary tree is the underlying tree of a unique rectangular Baxter TLT, that is to say a TLT with rectangular shape and which avoids the patterns  $\begin{smallmatrix} \blacksquare & \blacksquare \\ \blacksquare & \blacksquare \end{smallmatrix}$  and  $\begin{smallmatrix} \blacksquare & \blacksquare \\ \blacksquare & \blacksquare \end{smallmatrix}$ .*

We point out that a detailed study of TLTs with rectangular shapes (or alternatively of TLTs where we forget the underlying Ferrers diagram) is provided in [4], where these objects are referred to as *non-ambiguous trees*.

*Proof.* Consider a binary tree  $B$ , and denote by  $B_\ell$  (resp.  $B_r$ ) the left (resp. right) subtree pending from the root of  $B$ :  $B = \begin{matrix} \bullet \\ / \quad \backslash \\ B_\ell \quad B_r \end{matrix}$ . By induction (the base case of

the induction, which corresponds to a tree with just one vertex, being clear), there are unique Baxter TLTs of rectangular shapes, denoted  $T_\ell$  and  $T_r$ , whose underlying trees are respectively  $B_\ell$  and  $B_r$ . We are looking for a Baxter TLT  $T$  of rectangular shape whose underlying tree is  $B$ . Proposition 8 leaves us no choice but to place all points of  $T_\ell$  below and to the left of all points of  $T_r$ . That the resulting TLT (shown on the left of Figure 5) has a rectangular shape is ensured by the construction, and the avoidance of the two patterns is immediate to prove.  $\square$

Figure 5 (right) shows an example of rectangular Baxter TLT associated with a binary tree by Corollary 9.

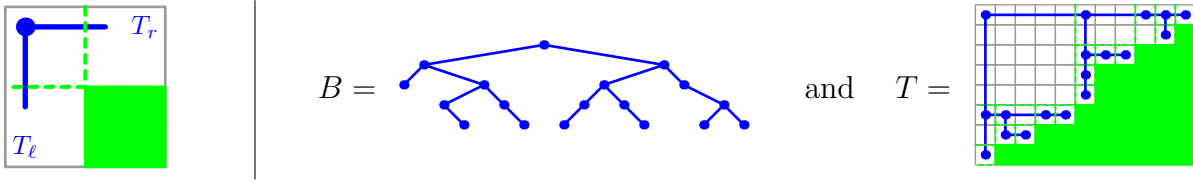


FIGURE 5. Left: Recursive construction of a TLT with rectangular shape. Right: A binary tree  $B$ , and the unique Baxter TLT  $T$  with rectangular shape whose underlying tree is  $B$ .

**Corollary 10.** *Let  $T$  be a Baxter TLT, and  $B$  be its underlying binary tree. Denote by  $B_\ell$  (resp.  $B_r$ ) the left (resp. right) subtree pending from the root of  $B$ . Consider the bipartition  $(L, R)$  of the non-root points of  $T$ , where  $L$  (resp.  $R$ ) contains all points of  $T$  that are in  $B_\ell$  (resp.  $B_r$ ).*

*We can split  $T$  with two lines  $\mathcal{V}$  and  $\mathcal{H}$ , uniquely defined by the following conditions:  $\mathcal{V}$  is a vertical line leaving all points of  $L$  to the left and all those of  $R$  to the right, and  $\mathcal{H}$  is a horizontal line leaving all points of  $L$  below and all those of  $R$  above.*

*Provided that both  $L$  and  $R$  are non-empty,  $\mathcal{V}$  and  $\mathcal{H}$  split  $T$  into four blocks, having the following properties.*

- *The Northwest block is a rectangle of empty cells, except for the North-westernmost cell, which contains the root of  $T$ .*



- The Southwest block is a Baxter TLT, denoted  $T_\ell$ , whose underlying tree is  $B_\ell$ .
- The Northeast block is a Baxter TLT, denoted  $T_r$ , whose underlying tree is  $B_r$ .
- The Southeast block is a Ferrers diagram, possibly empty, and contains only crossings of  $T$ .

*Proof.* The existence of  $\mathcal{V}$  and  $\mathcal{H}$  is guaranteed by Proposition 8. Their uniqueness is ensured by the fact that there are no empty rows nor columns in TLTs. The properties of the four blocks identified by  $\mathcal{V}$  and  $\mathcal{H}$  are immediate. We just note that the cells in the Southeast block are indeed crossings because they are all empty, have a point of  $R$  above them, and a point of  $L$  to their left (again, because every row and column of  $T$  contains at least one point).  $\square$

### 3. BIJECTION WITH PACKED FLOORPLANS

#### 3.1. Packed floorplans: Definition and basic properties.

**Definition 11** (Packed floorplans). A packed floorplan (PFP) of size  $(k, \ell)$  is a partition of a  $k \times \ell$  rectangle (i.e. a rectangle of height  $k$  and width  $\ell$ ) into  $k + \ell - 1$  rectangular tiles whose sides have integer lengths such that the pattern  $\lrcorner$  is avoided, meaning that: for every pair of tiles  $(t_1, t_2)$ , denoting  $(x_1, y_1)$  the coordinates of the bottom rightmost corner of  $t_1$  and  $(x_2, y_2)$  those of the top leftmost corner of  $t_2$ , it is not possible to have both  $x_1 \leq x_2$  and  $y_1 \geq y_2$ .

The set of packed floorplans of size  $(k, \ell)$  will be denoted by  $\mathcal{F}_{(k,\ell)}$ , and we set:  $\mathcal{F}_n = \bigsqcup_{k+\ell-1=n} \mathcal{F}_{(k,\ell)}$ .

Some examples and counter-examples of PFPs are provided by Figure 6, and Figure 7 shows all the packed floorplans of size 4. These PFPs are new combinatorial objects, but they are in size-preserving bijection with *mosaic floorplans* [1, 24, 30]. Indeed, as shown in the Appendix, mosaic floorplans are equivalence classes of objects, and PFPs are canonical representatives of mosaic floorplans.

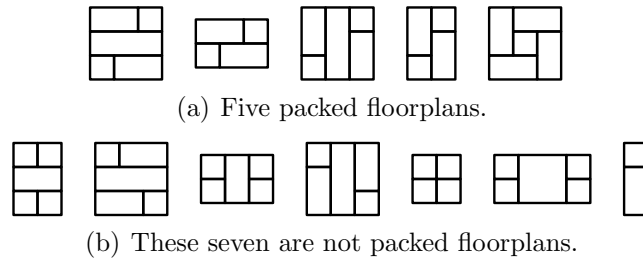


FIGURE 6. Some examples and counterexamples of PFPs.

Some properties of PFPs follow easily from Definition 11. We first introduce notation. A *T-junction* in a PFP  $F$  is a point where the sides of the tiles of  $F$  intersect in one of the following configurations:  $\top$ ,  $\perp$ ,  $\vdash$  and  $\dashv$ . A *segment* of a PFP  $F$  is a union of sides of tiles of  $F$  which forms a segment and which is maximal for this condition. Figure 8

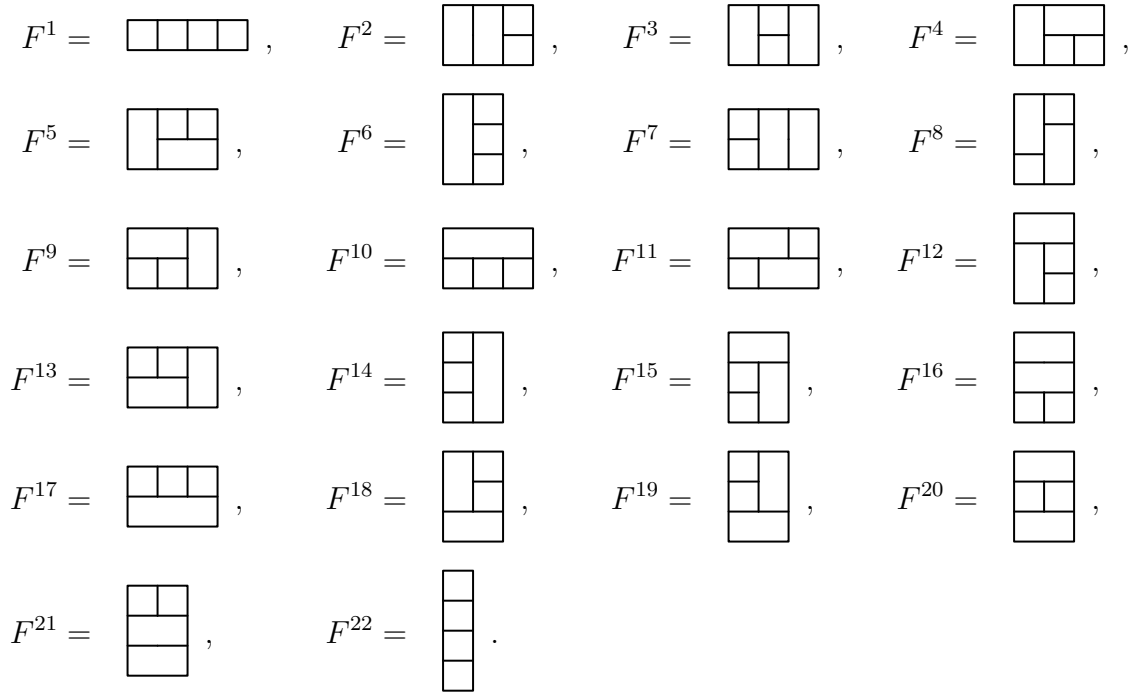
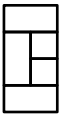


FIGURE 7. The 22 packed floorplans of size 4.

shows a PFP and its segments. A segment which is not a side of the bounding rectangle is called *internal*.



All the horizontal segments of this PFP are (from bottom to top)  $[(0, 0), (2, 0)]$ ,  $[(0, 1), (2, 1)]$ ,  $[(1, 2), (2, 2)]$ ,  $[(0, 3), (2, 3)]$  and  $[(0, 4), (2, 4)]$ . All its vertical segments are (from left to right)  $[(0, 0), (0, 4)]$ ,  $[(1, 1), (1, 3)]$  and  $[(2, 0), (2, 4)]$ .

FIGURE 8. A PFP of size  $(4, 2)$  and its segments.

**Observation 12.** Let  $F$  be a PFP.

- (i) Every corner of any of the tiles of  $F$  either is a corner of the bounding rectangle of  $F$  or forms a T-junction.
- (ii) Every horizontal (resp. vertical) line of integer coordinate included in the bounding rectangle of  $F$  contains exactly one segment of  $F$ .
- (iii) Every horizontal (resp. vertical) line of integer coordinate included in the bounding rectangle of  $F$  (except the bottom (resp. right) boundary of the bounding rectangle of  $F$ ) contains the top left corner of at least one tile of  $F$ .

*Proof.* For the first item, assume there exists a corner of a tile which neither is a corner of the bounding rectangle of  $F$  nor forms a T-junction. So, at this corner, either two or

four tiles meet. In the first (resp. second) case, there exists then two tiles  $t$  and  $t'$  placed as  $\begin{array}{c} t' \\ \lrcorner \\ t \end{array}$ , up to rotation (resp.  $\begin{array}{c} t' \\ \ulcorner \\ t \end{array}$ ). In both cases, we derive a contradiction. For the first case,  $t$  creates an inner corner in  $t'$ , hence  $t'$  is not of rectangular shape. In the second case, the pair of tiles  $(t', t)$  forms an occurrence of the pattern  $\lrcorner$ , which should be avoided.

We prove the second item in two steps. First, we show that each line contains at most one segment. This is clearly true for the boundaries of the bounding rectangle, which are obviously segments themselves. Consider an internal line, that is to say a line which is not a boundary of the bounding rectangle, and assume it contains at least 2 segments  $s$  and  $s'$ . If  $s$  and  $s'$  lie on the same horizontal (resp. vertical) line, with  $s$  to the left of (resp. above)  $s'$ , then because of (i) the right (resp. bottom) end of  $s$  is a T-junction  $\dashv$  (resp.  $\perp$ ) and the left (resp. top) end of  $s'$  is a T-junction  $\vdash$  (resp.  $\top$ ). Consider the tile  $t$  whose bottom right corner is the right (resp. bottom) end of  $s$ , and the tile  $t'$  whose top left corner is the left (resp. top) end of  $s'$ . The pair  $(t, t')$  forms a pattern  $\lrcorner$ , a contradiction.

Next, we show that a PFP  $F$  of size  $(k, \ell)$  contains exactly  $k + \ell + 2$  segments. Since this is also the number of lines considered in (ii), it follows from our first step that each of them contains *exactly* one segment. Denote by  $n_c$  (resp.  $n_t, n_j, n_s$ ) the number of corners of tiles (resp. of tiles, of T-junctions, of segments) of  $F$ . Each tile having 4 corners, we have  $4n_t = n_c$ . Also, from item (i), and since there are exactly two corners of tiles at any T-junction,  $n_c = 2n_j + 4$ . It follows that  $n_j + 2 = 2n_t$ . On the other end, every horizontal (resp. vertical) internal segment connects T-junctions of the form  $\vdash$  and  $\dashv$  (resp.  $\top$  and  $\perp$ ). And every T-junction is an end of a segment. It follows that  $n_j$  is twice the number of internal segments, which is  $n_s - 4$  taking into account the boundaries of the bounding rectangle of  $F$ . So,  $n_j = 2(n_s - 4)$ . Combining this equality with  $n_j + 2 = 2n_t$  obtained earlier gives  $n_t = (n_s - 4) + 1 = n_s - 3$ . Since  $F$  is a PFP of size  $(k, \ell)$ , it contains  $n_t = k + \ell - 1$  tiles, and it follows that  $n_s = k + \ell + 2$  as wanted.

Finally, the third item follows easily from the second one. Indeed, every line as in (iii) contains one segment. This segment, if horizontal (resp. vertical) is the support of the top (resp. left) side of at least one tile  $t$ , so it contains the top left corner of  $t$ .  $\square$

Our goal in this section is to describe a simple size-preserving bijection between Baxter TLTs and PFPs. The definition of our map  $\Phi_{\mathcal{F}}$  from  $\mathcal{T}_n$  to  $\mathcal{F}_n$  is given in Subsection 3.2. All that is needed to define it is the numbering of the points of TLTs induced by the procedure *RemovePoint*, and reviewed in Section 2. The proof that  $\Phi_{\mathcal{F}}$  is a bijection requires a few more properties of TLTs and PFPs. These are presented in Subsection 3.3, and allow to describe the inverse of  $\Phi_{\mathcal{F}}$ , proving that it is indeed a bijection.

**3.2. Definition of  $\Phi_{\mathcal{F}} : \mathcal{T}_n \rightarrow \mathcal{F}_n$ .** More precisely, we define  $\Phi_{\mathcal{F}} : \mathcal{T}_{(k,\ell)} \rightarrow \mathcal{F}_{(k,\ell)}$ , for all  $k, \ell$ .

Let us consider  $T \in \mathcal{T}_{(k,\ell)}$ . As noticed earlier,  $T$  contains  $n = k + \ell - 1$  points. These may be labeled by the integers in  $\{1, \dots, n\}$  according to the insertion procedure of [3], as explained in Section 2. We shall construct  $\Phi_{\mathcal{F}}(T)$  as follows.

We start from a rectangular  $k \times \ell$  box. We identify the unit cells of this box with the cells of  $T$ . For each label  $j = n, \dots, 1$ , we iteratively add a tile, the largest possible, whose top leftmost cell  $c$  is the one containing the point labeled by  $j$  in  $T$  (this tile is also said to have label  $j$ ). To build this largest possible tile, we only have to draw two segments: one vertical and one horizontal, each starting from the cell  $c$  and going respectively to the South and to the East. We denote the result by  $\Phi_{\mathcal{F}}(T)$ . See Figure 9 for an example.

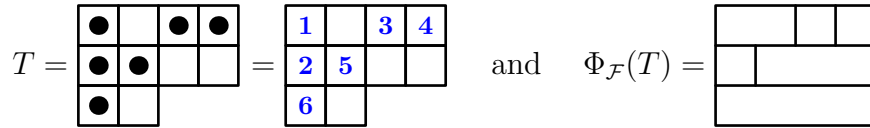


FIGURE 9. The bijection  $\Phi_{\mathcal{F}}$ .

**Proposition 13.** *The mapping  $\Phi_{\mathcal{F}} : \mathcal{T}_{(k,\ell)} \rightarrow \mathcal{F}_{(k,\ell)}$  is well-defined.*

*Proof.* Let  $T \in \mathcal{T}_{(k,\ell)}$ . Applying the above described construction, we obtain a tiling of a  $k \times \ell$  rectangle by  $n = k + \ell - 1$  tiles. So, to check that the mapping  $\Phi_{\mathcal{F}}$  is well-defined, we are just left with checking that at each step the tile we construct is actually of rectangular shape, and that the pattern  $\begin{smallmatrix} \blacksquare & \blacksquare \\ \blacksquare & \blacksquare \end{smallmatrix}$  is avoided.

First assume that some tile is not of rectangular shape, *i.e.*, has an inside corner (note that it has to be an inside SE corner because the tiles are added the largest possible). Denote by  $q$  the point of  $T$  in the top leftmost corner of this tile,  $c$  the point of  $T$  that creates the inside corner, and  $p$  the parent of  $c$  in  $T$  (see Figure 10(a)). Denoting  $(X(z), Y(z))$  the Cartesian coordinates of any point  $z$ , this means that either  $X(c) = X(p)$  and  $Y(c) < Y(p)$ , or  $Y(c) = Y(p)$  and  $X(c) > X(p)$ . In the former (resp. latter) case, we claim that  $Y(q) < Y(p)$  (resp.  $X(p) < X(q)$ ). Indeed, assuming the contrary, the insertion procedure of [3] would insert the points  $q$ ,  $p$ , and  $c$  in this order, contradicting that  $c$  is an inside corner of a tile. From these inequalities, we deduce that the points  $q$ ,  $p$ , and  $c$  form a pattern  $\begin{smallmatrix} \blacksquare & \blacksquare \\ \blacksquare & \blacksquare \end{smallmatrix}$  (resp.  $\begin{smallmatrix} \blacksquare & \blacksquare \\ \blacksquare & \blacksquare \end{smallmatrix}$ ) contradicting that  $T \in \mathcal{T}_{(k,\ell)}$ .

Suppose now that there are two tiles  $t_1$  and  $t_2$  that form a pattern  $\begin{smallmatrix} \blacksquare & \blacksquare \\ \blacksquare & \blacksquare \end{smallmatrix}$ . Let us choose this pair such that the distance between the bottom rightmost corner of  $t_1$  and the top leftmost corner of  $t_2$  is minimal. By construction, there is a point  $c$  of  $T$  in the top leftmost corner of  $t_2$ . Also, because  $t_1$  is constructed as large as possible, there is a point  $q$  (resp.  $u$ ) of  $T$  immediately outside  $t_1$  along its bottom (resp. right) border (see Figure 10(b)).

Denote by  $p$  the parent of  $c$  in  $T$ . We have  $X(c) = X(p)$  and  $Y(c) < Y(p)$ , or  $Y(c) = Y(p)$  and  $X(c) > X(p)$ . In the former (resp. latter) case, assume that  $Y(p) \leq Y(q)$  (resp.  $X(p) \geq X(u)$ ). Then  $t_1$  and the tile whose top leftmost corner is  $p$  would form a pattern  $\begin{smallmatrix} \blacksquare & \blacksquare \\ \blacksquare & \blacksquare \end{smallmatrix}$ , contradicting the minimality of  $(t_1, t_2)$ . Hence, we have  $Y(p) > Y(q)$  (resp.

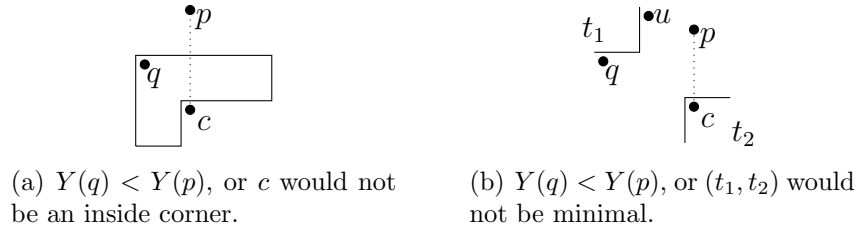


FIGURE 10. Illustrating the proof by contradiction that  $\Phi_{\mathcal{F}}(T) \in \mathcal{F}_{(k,\ell)}$ .

$X(p) < X(u)$ ), so that  $p, q, c$  (resp.  $p, u, c$ ) form a pattern  $\begin{smallmatrix} \bullet & \\ \bullet & \end{smallmatrix}$  (resp.  $\begin{smallmatrix} \bullet & \bullet \\ \bullet & \bullet \end{smallmatrix}$ ), contradicting that  $T \in \mathcal{T}_{(k,\ell)}$ .  $\square$

**3.3. Bijection between TLTs and packed floorplans.** The goal of the remainder of this section is to prove the following:

**Theorem 14.** *For any  $n$ ,  $\Phi_{\mathcal{F}}$  is a bijection between  $\mathcal{T}_n$  and  $\mathcal{F}_n$ .*

We start with a property on the (tree) structure of packed floorplans. From now on we will use the term *corner* for “top leftmost corner” (*i.e.*, NW-corner).

**Lemma 15.** *Let  $F$  be a PFP. The set of (top leftmost) corners of the tiles of  $F$  has a tree structure: for any corner  $c$  (different from the top leftmost corner of the bounding box), there exists another corner  $c'$  either above  $c$  or to its left, but not both.*

*Proof.* Let us consider the corner  $c$  of a tile  $t$ , different from the top leftmost tile of  $F$ . By Observation 12 (i), the corner  $c$  has to be either a  $\vdash$  or a  $\top$ . In the first case, the tile above  $t$  with common left side has its corner above  $c$ . If there were a corner  $c_1$  to the left of  $c$ , then there would exist another segment supported by the same line as the top edge of  $c$ , in contradiction with Observation 12 (ii). This proves our statement in the first case, and a symmetric argument applies to the second case.  $\square$

Next, we define an order on the tiles of PFPs.

**Definition 16.** *Let  $F \in \mathcal{F}_n$ . We define the tile-order of  $F$  as the labeling of the tiles obtained in the following way. We label the tiles from  $n$  to 1. After assigning the labels  $n, \dots, k+1$ , we label with  $k$  the tile which is the rightmost among the unlabeled tiles whose bottom border does not touch any unlabeled tile (equivalently, its bottom border touches only labeled tiles or the bottom border of the bounding rectangle).*

[include a figure to illustrate the tile-order.](#)

We shall now give another definition of the labeling of the pointed cells in a (Baxter) TLT,  $T$ , which is easily seen to be equivalent to the one given in Section 2. Indeed, the labeling of  $T$  is closely related to the tile-order of  $\Phi_{\mathcal{F}}(T)$ , and this is better seen on this equivalent definition of the labels of  $T$ .

**Definition 17.** *Let  $T \in \mathcal{T}_n$ . We define the point-order of  $T$  as follows. We label the pointed cells from  $n$  to 1. After assigning the labels  $n, \dots, k+1$ , we label with  $k$  the point*

which is the rightmost among those with no cells below it. If there is a cell to its right, we consider the ribbon of cells up to encountering a pointed cell, and we declare all cells of this ribbon “dead”. And in any case, we also declare “dead” the newly labeled pointed cell, and its empty row or column. Dead cells should be ignored (i.e., treated as if they did not exist) in later iterations of this labeling procedure.

**Observation 18.** *For a given pointed cell  $c$  with label  $j$ , any pointed cell  $c'$  which is weakly to the right and below  $c$  has a label  $j' > j$ .*

We now define an application  $\Psi_{\mathcal{F}}$ , which we will prove to be the inverse of  $\Phi_{\mathcal{F}}$ .

Let  $F \in \mathcal{F}_n$ . We associate to each tile a label  $k \in \{1, \dots, n\}$  using the tile-order, and we will construct a TLT  $T = \Psi_{\mathcal{F}}(F)$  with the pointed cells at the same positions as the corners of the tiles of  $F$ . Let us denote by  $U$  the object under construction. We start with  $U = \emptyset$ , and for  $k = 1, \dots, n$ :

- (1) we add a pointed cell to  $U$  at the same position as the corner of the tile labeled by  $k$  in  $F$ ;
- (2) we complete in such a way that the shape of  $U$  is still a Ferrers diagram (that is we add empty cells to the NW of the added pointed cell);
- (3) if the pointed cell labeled  $k$  is to the left of the pointed cell labeled  $k - 1$ , we place a ribbon from  $k$  to  $k - 1$ .

After dealing with  $n$ , we let  $T := U$ .

Given the insertion of ribbons in the last item above, a straightforward induction allows to prove the following observation.

**Observation 19.** *In the computation of  $\Psi_{\mathcal{F}}(F)$ , after dealing with the tiles labeled 1 to  $j$ , the latest pointed cell added (i.e., the pointed cell with label  $j$  for the tile-order) is the rightmost among the pointed cell without any cell below it.*

**Proposition 20.** *For any  $F \in \mathcal{F}_n$ ,  $\Psi_{\mathcal{F}}(F)$  is in  $\mathcal{T}_n$ .*

*Proof.* Let  $F \in \mathcal{F}_n$ , and  $T := \Psi_{\mathcal{F}}(F)$ . By construction, the shape of  $T$  is a Ferrers diagram. Because the position of the pointed cells in  $T$  corresponds to the position of the corners in  $F$ , Lemma 15 implies that any pointed cell (with the exception of the root) has either a pointed cell above it or to its left but not both. Observation 12(iii) implies that any row or column contains at least one pointed cell. Since the sizes clearly match,  $T$  is a TLT of size  $n$ .

To conclude the proof, it is enough to show that if  $T$  contains  $\begin{array}{|c|c|} \hline \bullet & \bullet \\ \hline \bullet & \bullet \\ \hline \end{array}$  or  $\begin{array}{|c|} \hline \bullet \\ \hline \bullet \\ \hline \end{array}$ , then  $F$  contains  $\lrcorner$ . So, assume  $T$  contains  $\begin{array}{|c|} \hline \bullet \\ \hline \bullet \\ \hline \end{array}$  (the other case being similar). Consider an occurrence of  $\begin{array}{|c|} \hline \bullet \\ \hline \bullet \\ \hline \end{array}$  in  $T$  where the distance between the two vertically aligned points of this occurrence is minimal. This implies that the topmost of these two points (denoted  $p$ ) is the parent of the bottommost one (denoted  $c$ ). By assumption, we know that there exists a point  $q$  to the left of  $p$  and  $c$ , which lies vertically between these two points. Consider the topmost  $q$  among all such points. Denote by  $t_1$  the tile of  $F$  whose bottom side is supported by the same segment as the top side of the tile containing  $q$ . And denote by  $t_2$

the tile containing  $c$ . We claim that  $t_1$  and  $t_2$  form a  $\lrcorner$  pattern. Indeed, if it were not the case, we would obtain a contradiction, either with the choice of  $q$  as topmost or with the fact that  $t_1$  is of rectangular shape (the tile containing  $p$  then creating an inner corner in  $t_1$ ).  $\square$

The following lemma is crucial in our proof of Theorem 14.

**Lemma 21.** *Let  $F$  be an element of  $\mathcal{F}_n$ . Let us denote by  $t$  and  $t'$  two tiles in  $F$ , with respective corners  $c$  and  $c'$  and respective labels  $i$  and  $j$  according to the tile-order. The following assertions are equivalent:*

- (1)  $c$  is (strictly) to the left and below  $c'$  and  $i = j + 1$ ;
- (2) the upper side of  $t$  and the lower side of  $t'$  are supported by the same segment, the  $T$ -junction at the bottom-left corner of  $t'$  is of the form  $\perp$ , and the right sides of  $t$  and  $t'$  form a  $\dashv$  (see Figure 11 (left)).



FIGURE 11. Left: The (tile-)ribbon configuration on packed floorplans. Right: Illustrating the proof of Lemma 21.

By analogy between Lemma 21 and Observation 3, we shall say that the configuration described by 2 is a *tile-ribbon* configuration for  $t$  and  $t'$ .

*Proof.* Let us prove that 2 implies 1. The configuration of the tiles  $t$  and  $t'$  implies that  $c$  is (strictly) to the left and below  $c'$ . Moreover, when building the tile-order on  $F$ , after giving the label  $i$  to the tile  $t$ , the tile  $t'$  becomes the rightmost among the tiles whose bottom border does not touch any unlabeled tile. Hence  $j = i - 1$ .

Conversely, let us prove that 1 implies 2. Since  $c'$  is to the right of  $c$  and  $j = i - 1$ , the bottom border of  $t'$  has to be in contact with  $t$  (otherwise it should be labeled first, *i.e.*, we would have  $j > i$ ). Thus the upper side of  $t$  and the lower side of  $t'$  are supported by the same segment, and the  $T$ -junction at the bottom-left corner of  $t'$  is of the form  $\perp$ . Since  $j = i - 1$ , the tile  $t'$  is the next one to be considered after  $t$  when building the tile-order. Thus  $t'$  is the rightmost tile such that the upper side of  $t$  and the lower side of  $t'$  meet forming a  $\perp$  in the bottom-left corner of  $t'$ . Moreover, the  $T$ -junction at the NE-corner of  $t$  has to be a  $\dashv$ : indeed, a  $\top$  would give a forbidden pattern together with the  $\perp$  of the SW-corner of  $t'$  (see Figure 11 (right)).  $\square$

**Lemma 22.** *Let  $T \in \mathcal{T}_n$  and  $F = \Phi_{\mathcal{F}}(T)$ . When identifying the pointed cells of  $T$  and the corners of the tiles of  $F$ , the point-order of  $T$  coincides with the tile-order of  $F$ .*

*Proof.* Assume that the orders coincide for labels  $n, \dots, k+1$ , but that the tile  $t$  of  $F$  with tile-label  $k$  corresponds to a point of  $T$  with point-order  $\ell-1$  for some  $\ell \leq k$ . Let  $c$  be this point with point-order  $\ell-1$ . In addition, denote by  $c'$  the point of  $T$  with point-order  $\ell$ , and by  $t'$  the tile of  $F$  whose corner is  $c'$ . Note that the tile-order of  $t'$  is at most equal to  $k$ .

We distinguish cases depending on the relative position of  $c$  and  $c'$ . In each case, we shall derive a contradiction, hence proving the lemma.

*Case 1:  $c$  is (weakly) below and to the right of  $c'$ .* Given that  $c$  and  $c'$  have respective labels  $\ell-1$  and  $\ell$ , Observation 18 immediately provides a contradiction.

*Case 2:  $c$  is above and to the right of  $c'$ .* We readily check that  $c'$  and  $c$  satisfy the first item of Lemma 21. Therefore, this lemma guarantees that the bottom edge of  $t$  is entirely supported by the top edge of  $t'$  (see Figure 11 (left), with  $t$  and  $t'$  exchanged w.r.t. the notation in this figure). This contradicts that, at step  $k$  in the computation of the tile-order,  $t$  is the rightmost among the unlabeled tiles whose bottom border does not touch any unlabeled tile (indeed,  $t'$  is unlabeled at this step).

*Case 3:  $c$  is above and to the left of  $c'$ .* Because  $t$  is the rightmost among the unlabeled tiles whose bottom border does not touch any unlabeled tile,  $t$  must extend until below and to the right of  $t'$ , contradicting that  $t$  is of rectangular shape.

*Case 4:  $c$  is below and to the left of  $c'$ .* Recall that at step  $k$  in the computation of the tile-order,  $t$  is the rightmost among the unlabeled tiles whose bottom border does not touch any unlabeled tile. So, because  $t'$  is unlabeled at this step, and is to the right of  $t$ , the bottom edge of  $t'$  must be touching an unlabeled tile. We denote by  $t''$  the leftmost such tile, and by  $c''$  its corner. To avoid the occurrence of a forbidden pattern in  $F$ , it is necessary that either the right edges of  $t'$  and  $t''$  are supported by the same segment, or their left edges are (or both). In the first case, Lemma 21 ensures that the point-order of  $c''$  is larger than the point-order of  $c'$ ; this also holds in the second case simply by definition of the point-order.

Note that  $t''$  is also unlabeled. If  $c''$  is to the right of  $c$ , we repeat this reasoning with  $t''$  instead of  $t'$ , and we iterate this procedure. This defines a sequence of points  $(c_1 = c', c_2 = c'', \dots, c_h)$ , where  $c_h$  is the corner of  $t_h$ , defined as the last unlabeled tile so reached (considering  $t$  among the unlabeled tiles). By the above remarks, the point-order is increasing along this sequence. Recalling that  $c'$  has point-order  $\ell$  and  $c$  has point-order  $\ell-1$ , we will reach a contradiction by showing that there exists an index  $j \leq h$  such that the point-order of  $c$  is at least that of  $c_j$ . To prove this, we exhibit an index  $j$  such that  $c_j$  is (weakly) above and to the left of  $c$ . (Indeed, the definition of the labeling of the points of a TLT then ensures that the point-order of  $c$  is at least that of  $c_j$ .)

Because the construction of the sequence  $(c_1, c_2, \dots, c_h)$  stops at  $c_h$ , it holds that  $c_h$  is (weakly) to the left of  $c$  or that  $t_h$  has its bottom border which does not touch any unlabeled tile. In this second case, by definition of  $t$ , it also holds that  $c_h$  is (weakly) to the left of  $c$ . This allows to define  $j$  as the smallest index such that  $c_j$  is (weakly) to the left of  $c$ . To conclude, we want to ensure that  $c_j$  is (weakly) above  $c$ . Since  $c_1 = c'$  is to the right of  $c$ , we know that  $c_{j-1}$  exists and is to the right of  $c$ , and that  $t_j$  and  $t_{j-1}$  have their right edges supported by the same segment, but not their left edges. Because  $t$  is labeled



before  $t_j$ , this leaves no other choice but to have  $c$  (weakly) below and to the right of  $c_j$ , concluding the proof.  $\square$

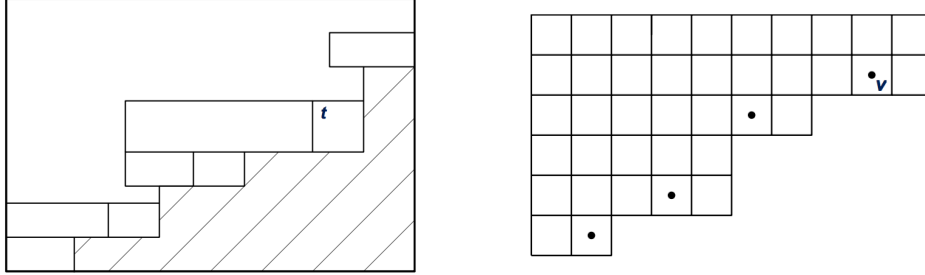


FIGURE 12. Illustrating the proofs of Lemmas 22 (left) and 23 (right).

La partie gauche de la figure n'est plus d'actualité. La remplacer par ce qui semble nécessaire à la lecture de la nouvelle preuve en 4 cas.

**Lemma 23.** *Let  $F \in \mathcal{F}_n$  and  $T = \Psi_{\mathcal{F}}(F)$ . When identifying the pointed cells of  $T$  and the corners of the tiles of  $F$ , the point-order of  $T$  coincides with the tile-order of  $F$ .*

*Proof.* This is a consequence of the definition of  $\Psi_{\mathcal{F}}$  and can be proved by induction. Note first that Observation 19 (applied for  $j = n$ ) ensures that the tile of  $F$  with label  $n$  and the point of  $T$  with label  $n$  coincide.

Now, let us suppose that the point-order in  $T$  coincides with the tile-order of  $F$  for labels  $n, \dots, k$ . We shall prove that they also coincide for label  $k - 1$ .

Let us consider the TLT, denoted  $\hat{T}$ , obtained by removing the cells of labels  $n, \dots, k$  from  $T$ , with the procedure *RemovePoint*. On the other hand, consider the object  $\tilde{F}$  obtained from  $F$  by keeping only the tiles of tile-label strictly less than  $k$ . Observe that  $\tilde{F}$  is not a PFP, since it is not of rectangular shape. We can nevertheless apply to  $\tilde{F}$  the same construction as in the definition of  $\Psi_{\mathcal{F}}$ , obtaining a TLT  $\tilde{T}$ . By definition of  $\Psi_{\mathcal{F}}$ , we have that  $\tilde{T} = \hat{T}$ . Consider the tile labeled by  $k - 1$  in  $\tilde{F}$  and the corresponding pointed cell in  $\tilde{T}$ , denoted  $c$ . (So,  $c$  has label  $k - 1$  for the tile-order.) Because of Observation 19,  $c$  is the rightmost of the pointed cell without any cell below it. In other words, it is the special point of  $\tilde{T}$ . Thus it gets the label  $k - 1$  for the point-order, as required.  $\square$

We shall now conclude the proof of Theorem 14.

*Proof of Theorem 14.* We can now conclude that the two applications  $\Psi_{\mathcal{F}}$  and  $\Phi_{\mathcal{F}}$  are inverse.

Indeed, let us consider  $T \in \mathcal{T}_n$ . We have proved that  $\Phi_{\mathcal{F}}(T)$  is in  $\mathcal{F}_n$ , thus we may define  $T' = \Psi_{\mathcal{F}}(\Phi_{\mathcal{F}}(T))$ . By definition of  $\Psi_{\mathcal{F}}$  and  $\Phi_{\mathcal{F}}$ , the pointed cells are the same in  $T$  and  $T'$ . Moreover, the point-order of these pointed cells coincide (Lemmas 22 and 23). Hence the ribbon configuration is the same in  $T$  and  $T'$ , which implies that  $T = T'$ . This proves that  $\Psi_{\mathcal{F}} \circ \Phi_{\mathcal{F}} = Id_{\mathcal{T}_n}$ .

We prove in the same way that  $\Phi_{\mathcal{F}} \circ \Psi_{\mathcal{F}} = Id_{\mathcal{F}_n}$ .  $\square$

4. BIJECTION WITH TWISTED BAXTER PERMUTATIONS

4.1. **A bijection between TLTs and permutations.** Recall that TLTs are in size-preserving bijection with permutations. Indeed, [3] provides several bijections between them. Here, we define yet another bijection between TLTs and permutations, which is however related to the so-called *code bijection* of [3] – see Proposition 26.

Consider a TLT  $T$  of size  $n$ . As described in Section 2, its pointed cells may be labeled by the integers  $1, \dots, n$ , by the insertion procedure. We now describe a way to extend this labeling to the empty cells of  $T$ . First, every empty cell  $c$  of the first column (resp. row) of  $T$  takes the label of the closest pointed cell above (resp. to the left of)  $c$  in the same column (resp. row). Notice that such a pointed cell always exists, because of the root of  $T$ . Second, we propagate this labeling to all empty cells of  $T$ , going from Northwest to Southeast, as follows. Consider an empty cell  $c$  that has not yet been labeled. Proceeding iteratively, we can assume that  $c$  has North, West, and Northwest neighboring cells in  $T$ , and that these have already been labeled. Denote by  $y$ ,  $z$  and  $x$  their respective labels (see Figure 13, left). We then distinguish four cases to determine the label of  $c$ :

- if there is a point above  $c$  in the same column, and a point to the left of  $c$  in the same row (recall that such cells are called *crossings*, a terminology that we will use again in Lemma 27), then  $c$  receives the label  $x$ ;
- if there is a point above  $c$  in the same column, but no point to the left of  $c$  in the same row, then  $c$  receives the label  $y$ ;
- if there is a point to the left of  $c$  in the same row, but no point above  $c$  in the same column, then  $c$  receives the label  $z$ ;
- if there is neither a point to the left of  $c$  in the same row, nor a point above  $c$  in the same column, then an easy induction ensures that  $x = y = z$ , and  $c$  receives this label.

Figure 13 (right) shows an example. We shall denote by  $\text{iso}(c)$  the label associated with the cell  $c$ .

Recall that we have defined another (partial) labeling, denoted  $\text{rib}$ , in Definition 5 (p. 5); note that it is defined for crossings  $c$  only, and that in general we have  $\text{iso}(c) \neq \text{rib}(c)$ .

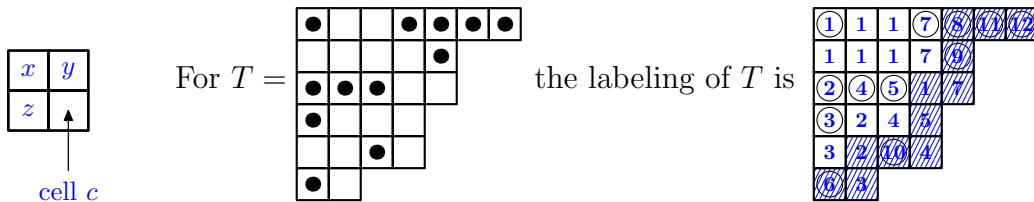


FIGURE 13. The iso-labeling of a TLT, which defines the bijection  $\phi$ . Our notational convention in the rightmost part of this figure is that pointed cells of the TLT are indicated by circled entries.

When all cells of  $T$  are labeled, we define  $\phi(T)$  as follows. Starting from the bottommost cell of the first column of  $T$ , we go along its Southeast border until the rightmost cell of

the first row of  $T$  is reached (that is to say, at every step, we go one cell to the right if this is a cell of the TLT, one cell up otherwise). Then  $\phi(T)$  is just the sequence of labels that are met along this Southeast border. For example, for the TLT  $T$  of Figure 13, we have  $\phi(T) = 632104517981112$ .

**Proposition 24.**  *$\phi$  is a size-preserving bijection between TLTs and permutations.*

Proposition 24 is an immediate corollary of Proposition 26 below. Its proof uses the following lemma:

**Lemma 25.** *Let  $T$  be a TLT of size  $n+1$  and  $T'$  be the TLT of size  $n$  (defined in Section 2) obtained from  $T$  by deletion of the special point  $s$  of  $T$  with its row (resp. column) and ribbon (if it exists). Let  $\sigma = \phi(T)$  and  $\sigma' = \phi(T')$ . Then the deletion of  $n+1$  in  $\sigma$  gives  $\sigma'$ . Moreover,  $n+1$  is located at the  $j$ -th position in  $\sigma$  where  $j$  is the number of cells (including  $s$  itself) along the border of  $T$  that are located at the Southwest of  $s$ .*

*Proof.* That  $n+1$  is located at the  $j$ -th position in  $\sigma$  is clear by definition of  $\phi$ . To prove that  $\sigma$  and  $\sigma'$  coincide up to the deletion of  $n+1$  in  $\sigma$ , let us examine how the labeling of all the cells of  $T$  (except  $s$ ) is related to the labeling of all the cells of  $T'$ .

Consider first the row (resp. column) of empty cells to the left of  $s$  (resp. above  $s$ ). The rules defining the labeling of  $T$  ensure that each such cell has the same label as the one immediately above it (resp. immediately to its left). As a consequence, all cells of  $T$  (except  $s$ ) that are neither in the row (resp. column) nor in the ribbon of  $s$  have the same label in  $T$  as in  $T'$ . The only labels yet to determine are those of the cells of the ribbon of  $s$ , when it exists. Because there are no empty rows nor columns, such a cell is always a crossing, hence it has the same label as its Northwest neighboring cell.

Whether or not the ribbon of  $s$  exists, we can now compare the labelings of  $T$  and  $T'$ . And it follows immediately that, up to  $n+1$  which corresponds to  $s$ , the sequence of integers defining  $\sigma$  that is read along the Southeast border of  $T$  is the same as the sequence read along Southeast border of  $T'$ , *i.e.*, is  $\sigma'$ .  $\square$

**Proposition 26.** *Denote by  $\Phi_1$  the code bijection of [3, Theorem 3.4] between TLTs and permutations. For any TLT  $T$ , denoting by  $\tau$  the permutation such that  $\Phi_1(T) = \tau^{-1}$ , we have  $\tau = \phi(T)$ .*

*Proof.* The proof is by induction on the size of  $T$ . The base case of the induction is clear. Let  $T$  be a TLT of size  $n+1$  and  $T'$  be the TLT of size  $n$  obtained from  $T$  by deletion of the special point  $s$  of  $T$  with its row (resp. column) and ribbon (if it exists). Consider the permutations  $\sigma = \phi(T)$ ,  $\sigma' = \phi(T')$ ,  $\tau = \Phi_1(T)^{-1}$  and  $\tau' = \Phi_1(T')^{-1}$ . By induction hypothesis,  $\sigma' = \tau'$ . Moreover, by Lemma 25,  $\sigma$  is obtained from  $\sigma'$  by insertion of  $n+1$  at position  $j$ , where  $j$  is the number of cells along the border of  $T$  that are located at the Southwest of  $s$ . From the definition of  $\Phi_1$  in [3], we have similarly that  $\tau$  is obtained from  $\tau'$  by insertion of  $n+1$  at the same position  $j$ . We deduce that  $\sigma = \tau$ , concluding the proof.  $\square$

**4.2. Labels of crossings in the bijection  $\phi$ .** In the labeling of the cells of a TLT  $T$  that defines the bijection  $\phi$ , the integers labeling the crossings of  $T$  have a nice interpretation

in the permutation  $\phi(T)$  – see Lemma 27. This interpretation is essential for the study of the specialization of  $\phi$  to Baxter objects, in Subsection 4.3. To explain it, we need to review the classical notions of vincular and bivincular patterns in permutations [8].

- A (*classical*) *pattern* is simply a permutation; but for notational convenience, we insert a dash between any two adjacent entries. An *occurrence* of a classical pattern  $\tau$  in a permutation  $\sigma$  is a subsequence of  $\sigma$  which is order-isomorphic to  $\tau$ .
- A *vincular pattern* (or *dashed pattern*) is a permutation in which every pair of adjacent entries may be linked by a dash. Occurrences of a vincular pattern  $\tau$  in a permutation  $\sigma$  are defined like in the case of classical patterns, with the additional restriction that two adjacent entries of  $\tau$  that are not separated by a dash must correspond to adjacent entries in  $\sigma$ .
- *Bivincular* patterns are a generalization of vincular patterns, where adjacency constraints are allowed not only on positions but also on values.

Here, we will be interested in very simple bivincular patterns, with only one constraint on values. Such patterns of size  $n$  can be represented as a vincular pattern whose entries are  $\{1, 2, \dots, n-1\} \cup \{i^+\}$ , for some  $i \in \{1, 2, \dots, n-1\}$ . In an occurrence of such a pattern in a permutation  $\sigma$ , we require that the entries of  $\sigma$  corresponding to  $i$  and  $i^+$  have consecutive values (namely, that  $i^+$  corresponds to  $k+1$  when  $i$  corresponds to  $k$ ). The (bivincular) pattern  $2^+ - 1 - 2$  will be of particular interest to us, so let us rephrase: An occurrence of a  $2^+ - 1 - 2$  pattern in a permutation  $\sigma$  is a subsequence  $\sigma(i)\sigma(j)\sigma(k)$  of  $\sigma$ , with  $i < j < k$  such that  $\sigma(j) < \sigma(k)$  and  $\sigma(i) = \sigma(k) + 1$ .

For example, consider the classical pattern  $3 - 1 - 2$ , the vincular pattern  $3 - 12$ , and the bivincular patterns  $2^+ - 1 - 2$  and  $2^+ - 12$ . Their occurrences in  $\sigma = 6\ 3\ 2\ 10\ 4\ 5\ 1\ 7\ 9\ 8\ 11\ 12$  are summarized in Figure 14. Notice that this permutation  $\sigma$  satisfies  $\sigma = \phi(T)$ , where  $T$  is the TLT of Figure 13.

$\tau$	Occurrences of $\tau$ in $\sigma$
$3 - 1 - 2$	6 3 4, 6 3 5, 6 2 4, 6 2 5, 6 4 5, 10 4 5, 10 4 7, 10 4 9, 10 4 8, 10 5 7, 10 5 9, 10 5 8, 10 1 7, 10 1 9, 10 1 8, 10 7 9, 10 7 8
$3 - 12$	6 4 5, 10 4 5, 10 1 7, 10 7 9
$2^+ - 1 - 2$	6 3 5, 6 2 5, 6 4 5, 10 4 9, 10 5 9, 10 1 9, 10 7 9
$2^+ - 12$	6 4 5, 10 7 9

FIGURE 14. Occurrences of several patterns in  $\sigma = 6\ 3\ 2\ 10\ 4\ 5\ 1\ 7\ 9\ 8\ 11\ 12$ .

**Lemma 27.** *The crossings of any TLT  $T$  are in one-to-one correspondence with the occurrences of the pattern  $2^+ - 1 - 2$  in  $\sigma = \phi(T)$ .*

*Under this correspondence, for any crossing  $c$ , the value of  $\sigma$  to which 1 is mapped is  $\text{iso}(c)$  defined in Subsection 4.1 and the value of  $\sigma$  to which  $2^+$  is mapped is  $\text{rib}(c)$  defined in Definition 5 (p. 5).*

*Proof.* The proof is by induction on the size of  $T$ , the base case of the induction being clear. Let  $T$  be a TLT of size  $n + 1$  and  $T'$  be the TLT of size  $n$  obtained from  $T$  by deletion of the special point  $s$  of  $T$  with its row (resp. column) and ribbon (if it exists).

The crossings of  $T$  are partitioned in two categories: the crossings of  $T'$  and the cells of the ribbon of  $s$ . As explained in Observation 6, note that all the cells of the ribbon of  $s$  are crossings.

Consider  $\sigma = \phi(T)$  and  $\sigma' = \phi(T')$ . From Lemma 25,  $\sigma'$  may be described as  $\sigma$  from which  $n + 1$  has been deleted. Hence, the occurrences of  $2^+ - 1 - 2$  in  $\sigma$  are also partitioned in two categories: the occurrences of  $2^+ - 1 - 2$  in  $\sigma'$  and those where  $2^+$  is mapped to  $n + 1$ .

By induction, it follows that the crossings of  $T'$  are mapped to the occurrences of  $2^+ - 1 - 2$  in  $\sigma'$ . The assertion about the values is readily checked, since for any such crossing  $c$  of  $T'$ ,  $\text{iso}(c)$  (resp.  $\text{rib}(c)$ ) is the same in  $T$  and in  $T'$ .

Consider now a crossing of  $T$  which is a cell of the ribbon of  $s$ . Recall that the label of  $s$  is  $n + 1$ . Observe now that the pointed cell located at the right extremity of the ribbon of  $s$  is the special point  $s'$  of  $T'$ , whose label is therefore  $n$ . From these observations, it is now clear that the occurrences of  $2^+ - 1 - 2$  where  $2^+$  is mapped to  $n + 1$  are in one-to-one correspondence with the cells of the ribbon of  $s$ . In this case, the assertion about the values follows immediately by definition of  $\text{iso}(\cdot)$  and  $\text{rib}(\cdot)$ .  $\square$

### 4.3. Specialization of this bijection on Baxter TLTs.

**Definition 28** (Twisted Baxter permutations). *A twisted Baxter permutation is a permutation  $\sigma$  which avoids the two vincular patterns  $2 - 41 - 3$  and  $3 - 41 - 2$  (i.e., such that none of these patterns has any occurrence in  $\sigma$ ). We denote by  $\mathcal{B}_n$  the set of inverses of twisted Baxter permutations of size  $n$ .*

**Observation 29.** *The permutations of  $\mathcal{B}_n$  may alternatively be characterized as the permutations of size  $n$  avoiding the patterns  $2^+ - 1 - 3 - 2$  and  $2^+ - 3 - 1 - 2$ , or equivalently the patterns  $3 - 14 - 2$  and  $3 - 41 - 2$ , i.e.,*

$$\mathcal{B}_n = \text{Av}_n(2^+ - 1 - 3 - 2, 2^+ - 3 - 1 - 2) = \text{Av}_n(3 - 14 - 2, 3 - 41 - 2).$$

*Proof.* When taking the inverse, the adjacency constraints in a vincular pattern are turned into constraints that two elements should have *consecutive values*, (which can be represented by a bivincular pattern). This proves the first statement of Observation 29.

The second statement of Observation 29 is proved using classical arguments of permutation patterns analysis. We prove that a permutation  $\sigma$  contains a pattern  $3 - 14 - 2$  if and only if it contains a pattern  $2^+ - 1 - 3 - 2$ , the case of  $3 - 41 - 2$  and  $2^+ - 3 - 1 - 2$  being similar.

Suppose that  $\sigma$  contains a pattern  $3 - 14 - 2$  where the 2 is mapped to the entry  $i$  and the 3 is mapped to the entry  $j$  of  $\sigma$ . We consider the integers in the interval  $\{i, \dots, j\}$ . They stand in  $\sigma$  either to the left or to the right of the subpattern 14, with  $j$  to the left and  $i$  to the right. Thus, considering these integers in decreasing order, there exist two

consecutive of them,  $k$  and  $(k+1)$  with  $i \leq k < j$ , which stand as:  $(k+1) \dots 14 \dots k$ . This gives a pattern  $2^+ - 1 - 3 - 2$ .

Conversely, if  $\sigma$  contains a pattern  $2^+ - 1 - 3 - 2$ , we consider the entries in the subword  $1 - 3$ . They are either strictly greater than  $2^+$  or smaller than 2, thus there are two of them which are at adjacent positions and form a pattern  $2^+ - 13 - 2$  and hence  $3 - 14 - 2$ .  $\square$

Figure 15 lists all permutations of  $\mathcal{B}_4$ .

$$\begin{aligned} \sigma^1 &= 1234, & \sigma^2 &= 1243, & \sigma^3 &= 1324, & \sigma^4 &= 1342, & \sigma^5 &= 1423, & \sigma^6 &= 1432, \\ \sigma^7 &= 2134, & \sigma^8 &= 2143, & \sigma^9 &= 2314, & \sigma^{10} &= 2341, & \sigma^{11} &= 2413, & \sigma^{12} &= 2431, \\ \sigma^{13} &= 3124, & \sigma^{14} &= 3214, & \sigma^{15} &= 3241, & \sigma^{16} &= 3421, & \sigma^{17} &= 4123, & \sigma^{18} &= 4132, \\ \sigma^{19} &= 4213, & \sigma^{20} &= 4231, & \sigma^{21} &= 4312, & \sigma^{22} &= 4321. \end{aligned}$$

FIGURE 15. The 22 permutations of  $\mathcal{B}_4$ .

There are several bijective proofs in the literature that  $|\mathcal{B}_n| = \text{Bax}_n$  for all  $n$ , or more precisely that (some symmetry of) twisted Baxter permutations are enumerated by Baxter numbers. See [19] for a recursive bijection between Baxter permutations and permutations avoiding  $2 - 14 - 3$  and  $3 - 14 - 2$  (whose reverses are twisted Baxter permutations), or [29, 17] for more recent bijections between Baxter permutations and twisted Baxter permutations. In these articles, the pattern-avoiding families of permutations are defined by the avoidance *barred* patterns rather than by excluded *dashed* patterns; but in each case the equivalence between both descriptions is easily proved, with simple arguments similar to those in the proof of Observation 29.

Let us denote by  $\Phi_{\mathcal{B}}$  the restriction of the bijection  $\phi$  of Subsection 4.1 to the set of Baxter TLTs.

Our goal is to prove the following:

**Theorem 30.** *For any  $n$ ,  $\Phi_{\mathcal{B}}$  is a bijection between  $\mathcal{T}_n$  and  $\mathcal{B}_n$ .*

This is an immediate consequence of the following proposition.

**Proposition 31.** *Let  $\sigma$  be a permutation, of size  $n$ , and  $T$  be the TLT defined by  $T = \phi^{-1}(\sigma)$ . Then  $\sigma \in \mathcal{B}_n$  if and only if  $T \in \mathcal{T}_n$ .*

*Proof.* The key point is Lemma 27. Let  $\sigma$  and  $T$  be as in the statement of the proposition, and consider the sequence of TLTs  $(T_n = T, T_{n-1} = T', T_{n-2}, \dots, T_1 = \blacksquare)$  defined in Section 2.

We first prove that if  $\sigma$  contains a pattern  $2^+ - 3 - 1 - 2$  or  $2^+ - 1 - 3 - 2$ , then  $T$  contains a pattern  $\begin{smallmatrix} \bullet & \bullet \\ \bullet & \bullet \end{smallmatrix}$  or  $\begin{smallmatrix} \bullet & \bullet & \bullet \\ \bullet & \bullet & \bullet \end{smallmatrix}$ . For this purpose, we consider the occurrence of one of the patterns  $2^+ - 3 - 1 - 2$  and  $2^+ - 1 - 3 - 2$  in  $\sigma$  such that the value  $j$  of the “ $2^+$ ” is maximal among all possibilities, and such that the value  $k$  of the “3” is minimal among these occurrences. From [3], this guarantees that the ribbon  $R$  from  $j$  (the “ $2^+$ ”) to  $j - 1$  (the “2”) is exactly the same in  $T_j$  and  $T_{k-1}$ . In  $T_k$ , the pointed cell labeled by  $k$  is either

to the South or to the East of a crossing which belongs to  $R$ , thus giving a pattern  $\begin{smallmatrix} \bullet & \bullet \\ \bullet & \bullet \end{smallmatrix}$  or  $\begin{smallmatrix} \bullet & \bullet \\ \bullet & \bullet \end{smallmatrix}$  pattern in  $T$ .

Conversely, we prove that if  $T$  contains a pattern  $\begin{smallmatrix} \bullet & \bullet \\ \bullet & \bullet \end{smallmatrix}$  or  $\begin{smallmatrix} \bullet & \bullet \\ \bullet & \bullet \end{smallmatrix}$ , then  $\sigma$  contains a pattern  $2^+ - 3 - 1 - 2$  or  $2^+ - 1 - 3 - 2$ . We consider the smallest  $i$  such that  $T_i$  contains a pattern  $\begin{smallmatrix} \bullet & \bullet \\ \bullet & \bullet \end{smallmatrix}$  or  $\begin{smallmatrix} \bullet & \bullet \\ \bullet & \bullet \end{smallmatrix}$ . The Southeasternmost point of this pattern in  $T_i$  is the special point  $s_i$  of  $T_i$  (because  $T_{i-1}$  avoids the two patterns). Moreover, it is to the South or to the East of a crossing of  $T_i$ , which we denote  $c$ . Let us denote  $\sigma_i = \phi(T_i)$ . We claim that  $\sigma_i$  contains a  $2^+ - 3 - 1 - 2$  or  $2^+ - 1 - 3 - 2$  pattern. Indeed, such a pattern can be identified using Lemma 27. More precisely, it is enough consider the entries of  $\sigma_i$  corresponding to the following cells of  $T_i$ : the pointed cell labeled  $iso(c)$  (which corresponds to the “1” in the pattern),  $s_i$  (which is the “3”) and the two extremities of the ribbon of  $c$  (which are the “2+” and “2”). To conclude, Lemma 25 implies that  $\sigma_i$  is a pattern of  $\sigma$ , so that  $\sigma$  also contains a  $2^+ - 3 - 1 - 2$  or  $2^+ - 1 - 3 - 2$  pattern.  $\square$

Figure 16 shows an example of a Baxter TLT  $T$  with the corresponding permutation  $\Phi_B(T)$ .

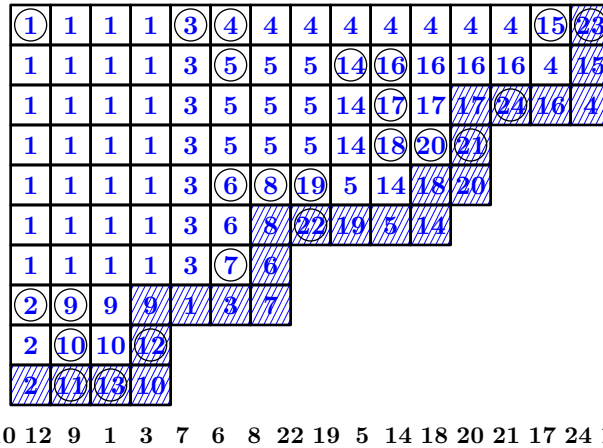
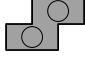


FIGURE 16. A Baxter TLT  $T$  (circled entries represent pointed cells), its labeling by  $iso(\cdot)$ , and the permutation  $\Phi_B(T)$ .


4.4.  $\Phi_B$  and classical permutation statistics. It is interesting to note that the iso-labeling of a Baxter TLT allows to interpret some classical statistics on the permutation  $\Phi_B(T)$  directly on the Baxter TLT  $T$ . We describe here these interpretations for the descents and the left-to-right minima.

4.4.1. *Descents.* Our notational convention in Figures 17 to 20 is that  $\textcircled{\bullet}$  or  $\bullet$  represents a pointed cell,  $\begin{smallmatrix} \square & \square \\ \square & \square \end{smallmatrix}$  is a region of empty cells,  $\begin{smallmatrix} \square & \square \\ \square & \bullet \end{smallmatrix}$  is a region of pointed and/or empty

cells, and  is a region of cells containing at least a point. Note that some regions contain only empty cells because of the excluded patterns that define Baxter TLTs.

**Lemma 32.** *Let  $T$  be a Baxter TLT. Let  $c$  be a (pointed or empty) cell of  $T$  that does not belong to the first column (resp. row) and without any pointed cell below it (resp. to its right). Denote by  $a$  the iso-label of  $c$  and by  $b$  the iso-label of the cell<sup>2</sup> immediately to the left of (resp. above)  $c$ . Then  $ba$  (resp.  $ab$ ) is a factor<sup>3</sup> of  $\sigma = \Phi_{\mathcal{B}}(T)$ .*

*Proof.* If  $c$  is the bottom-most (resp. rightmost) cell in its column (resp. row), then the claim immediately holds by definition of  $\Phi_{\mathcal{B}}$ . Otherwise, we prove that the cell immediately below (resp. to the right) of  $c$  satisfies the same conditions as  $c$ , induction giving then the conclusion.

Suppose that  $c$  does not belong to the first column and has no pointed cell below it. Consider the cell immediately below  $c$ , denoted  $c'$ . Note that our assumptions ensure that  $c'$  is empty. Two cases may occur, as shown on Figure 17 (left): either there is no pointed cell to the left of  $c'$ , or there is at least one. In the first case,  $c'$  has no pointed cell below it, is labeled by  $a$  and the cell to its left by  $b$ , so that we can proceed inductively, and obtain that  $ba$  is a factor of  $\sigma$ . In the second case, let us first notice that there is at least a point above  $c'$  (since the column of  $c'$  contains at least a point). This implies that there is no point to the right of  $c'$  in its row (or otherwise, we would obtain a pattern , with a point above  $c'$  and two points to the left and right of  $c'$ ). This also implies that the label of  $c'$  is  $b$  (by the first case of the rule for the propagation of the iso-label). The cell above  $c'$  is nothing but our original cell  $c$ , so it is labeled by  $a$ . We can therefore apply our inductive statement on  $c'$ , obtaining that  $ba$  is a factor of  $\sigma$ .

In the case where  $c$  does not belong to the first row and has no pointed cell to its right, we proceed similarly, distinguishing cases as shown on Figure 17 (right).  $\square$

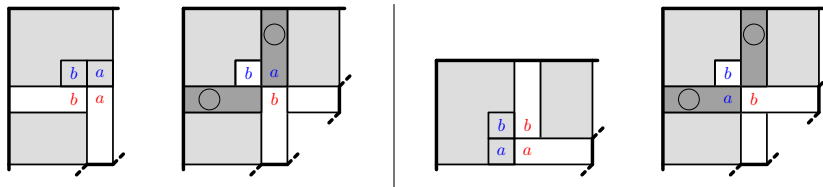


FIGURE 17. Proof of Lemma 32 when  $c$  has no pointed cell below it (left), and when  $c$  has no pointed cell to its right (right).

dans la deuxième et la quatrième figure, la case contenant le  $b$  bleu devrait être en grisé clair.

<sup>2</sup>Note that this cell exists, because of our assumption that  $c$  does not belong to the first column (resp. row).

<sup>3</sup>As in words, a *factor* in a permutation is a sequence of symbols which appear consecutively.



**Definition 33.** A point of a Baxter TLT is column-extremal (resp. row-extremal) if it does not belong to the first column (resp. row) and there is no pointed cell below it (resp. to its right).

The column-ancestor (resp. row-ancestor) of a column-extremal (resp. row-extremal) point  $x$  is the parent of the top-most (resp. left-most) point in the column (resp. row) of  $x$ .

Figure 18 illustrates this definition.

In Definition 33, note that the top-most (resp. left-most) point in the column (resp. row) of  $x$  is not the root of the TLT, since  $x$  does not belong to the first column (resp. row). This ensures that it has a parent so that column- and row-ancestors are well defined. Note also that the column-ancestor (resp. row-ancestor) of a column-extremal (resp. row-extremal) point  $x$  is located in a column to the left of  $x$  (resp. in a row above  $x$ ).

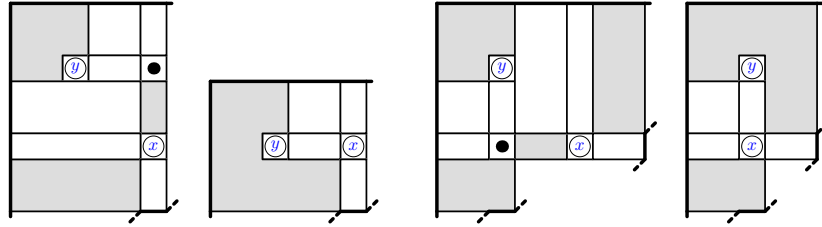


FIGURE 18. The column-ancestor (resp. row-ancestor)  $y$  of a column-extremal (resp. row-extremal) point  $x$  in a Baxter TLT, with the special case where  $x$  is the only point in its column (resp. row) shown on the right.

**Proposition 34.** In a Baxter TLT  $T$ , consider a column-extremal (resp. row-extremal) point  $x$  and its column-ancestor (resp. row-ancestor)  $y$ . Denote by  $a$  the label of  $x$  and by  $b$  the label of  $y$ . Then  $ba$  (resp.  $ab$ ) is a factor of  $\sigma = \Phi_{\mathcal{B}}(T)$  and forms an ascent (resp. descent) in  $\sigma$ .

*Proof.* First, we will see that the cell immediately to the left of (resp. above)  $x$  has iso-label  $b$ . Lemma 32 will then ensure that  $ba$  (resp.  $ab$ ) is a factor of  $\sigma$ . The claim we actually prove is a bit more general: it states that all the cells in the rectangle extending from  $y$  to the cell immediately to the left of (resp. above)  $x$  have iso-label  $b$ . (See Figures 19 and 20.)

Assume that  $x$  is a column-extremal point and that  $y$  is its column-ancestor, and consider the rectangle extending from  $y$  to the cell immediately to the left of  $x$ . This case is illustrated on Figure 19. For the cells of the top row of this rectangle, our claim follows easily from the third case defining the propagation of the iso-labels, since such cells have no point of  $T$  above them (or a pattern  $\begin{smallmatrix} \blacksquare & \blacksquare \\ \blacksquare & \blacksquare \end{smallmatrix}$  would be created). It is just as easy for the cells of the leftmost column of this rectangle, for which the second case of the propagation rule applies, since they have no point of  $T$  to their left (or a pattern  $\begin{smallmatrix} \blacksquare & \blacksquare \\ \blacksquare & \blacksquare \end{smallmatrix}$  would be created). For

the remaining cells of this rectangle, the last case of propagation rule applies, all together proving our claim.

The case where  $x$  is a row-extremal point and  $y$  is its row-ancestor is handled similarly, as shown by Figure 20.

Finally, the parent of any point  $x$  in an TLT has a label smaller than the one of  $x$ , and so do all ancestors of  $x$ . This proves that  $ba$  (resp.  $ab$ ) is an ascent (resp. descent) of  $\sigma$ .  $\square$

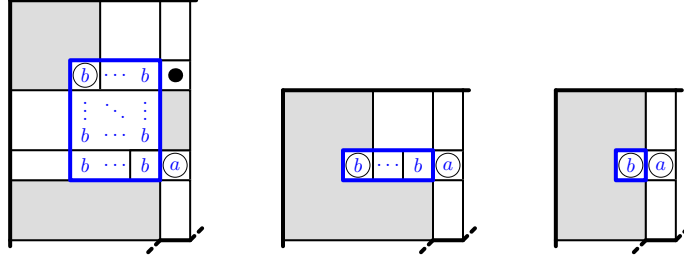


FIGURE 19. Propagation of the iso-label of the column-ancestor of a column-extremal point, in all possible configurations.

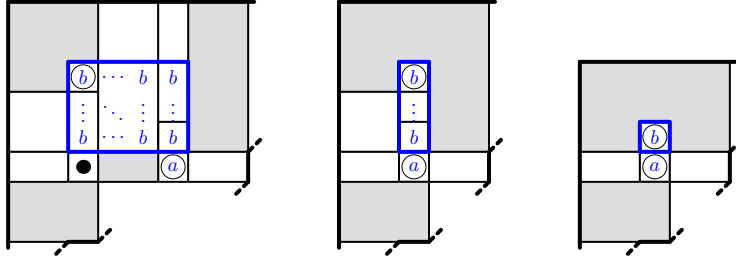


FIGURE 20. Propagation of the iso-label of the row-ancestor of a row-extremal point, in all possible configurations.

**Corollary 35.** *For a Baxter TLT  $T$ , all the ascents and descents of  $\sigma = \Phi_{\mathcal{B}}(T)$  are those described in Proposition 34.*

*Proof.* Denote by  $n$  the common size of  $T$  and  $\sigma$ . From Definition 7,  $T$  has in total  $n+1$  rows and columns, so that there are  $n-1$  distinct pairs  $(x, y)$  where  $x$  is a column-extremal (resp. row-extremal) point and  $y$  is its column-ancestor (resp. row-ancestor). Proposition 34 then gives  $n-1$  distinct factors of length 2 in  $\sigma$ , which are either ascents or descents as described in Proposition 34, so that the ascents and descents of  $\sigma$  are completely described.  $\square$

#### 4.4.2. Left-to-right minima.

**Proposition 36.** *Let  $T$  be a Baxter TLT, and denote by  $T_\ell$  and  $T_r$  the Baxter TLTs defined in Corollary 10 (p.8). Let  $\sigma = \Phi_{\mathcal{B}}(T)$ , and decompose  $\sigma$  around its minimum value*

as  $\sigma = \sigma_\ell 1 \sigma_r$ . The permutations  $\Phi_{\mathcal{B}}(T_\ell)$  and  $\Phi_{\mathcal{B}}(T_r)$  are order-isomorphic to the sequences  $\sigma_\ell$  and  $\sigma_r$  respectively.

*Proof.* The claim obviously holds when  $T_\ell$  or  $T_r$  is empty, so assume they are not.

Notice first that the points of  $T_\ell$  (resp.  $T_r$ ) may be equipped with two different labelings: one labeling is inherited from the labeling of the TLT  $T$ , and one is its own labeling as TLTs. These are not identical, but by construction, they are “order-isomorphic” (that is to say, the comparison between the labels of any two points is the same in both labelings).

Now, both labelings may be propagated following the rules of propagation of the iso-labeling, yielding two order-isomorphic labelings of the cells of  $T_\ell$  (resp.  $T_r$ ).

To conclude, it is enough to prove that  $\sigma_\ell$  (resp.  $\sigma_r$ ) is the word that is read along the Southeast border of  $T_\ell$  (resp.  $T_r$ ), in the iso-labeling propagated from the original labeling of  $T$ . And this claim holds because all cells in the Southeast block identified by Corollary 10 are crossings, and because the iso-labels of crossings are inherited following Northeast-Southwest diagonals.  $\square$

**Corollary 37.** *Let  $T$  be a Baxter TLT, and let  $\sigma = \Phi_{\mathcal{B}}(T)$ . The left-to-right minima of  $\sigma$  are the labels of the points of the left-most column of  $T$ .*

*Proof.* It follows easily from Proposition 36 by induction.

Given  $T$ , denote by  $T_\ell$  and  $T_r$  the Baxter TLTs defined in Corollary 10. Decompose also  $\sigma$  as  $\sigma_\ell 1 \sigma_r$  like in the statement of Proposition 36. The claim clearly holds when  $T_\ell$  is empty: indeed, the only point of  $T$  in the first column is the root of  $T$ , labeled by 1, and  $\sigma$  starts with 1. If  $T_\ell$  is not empty, the left-to-right minimal of  $\sigma$  are those of  $\sigma_\ell$  and 1. Induction ensures that the left-to-right minima of  $\sigma_\ell$  are the labels of the points in its first column. And 1 is the label of the root of  $T$ , which is the only point in the first column of  $T$  that is not in the first column of  $T_\ell$ .  $\square$

## 5. BIJECTION WITH NON-INTERSECTING LATTICE PATHS

**Definition 38** (Triples of non-intersecting lattice paths). *A triple of non-intersecting lattice paths of size  $n$  is a set of three lattice paths, with unitary  $N = (0, 1)$  and  $E = (1, 0)$  steps, that never meet, which respectively start at  $(1, 0)$ ,  $(0, 1)$  and  $(-1, 2)$  and end at  $(n - i, i)$ ,  $(n - i - 1, i + 1)$  and  $(n - i - 2, i + 2)$  for some  $i \in [0..(n - 1)]$  (thus each of the three paths has  $n - 1$  steps).*

*Let us denote by  $\mathcal{P}_n$  the set of triples of non-intersecting lattice paths of size  $n$ .*

Figure 24 (p. 31) (right) shows an example of triple of non-intersecting lattice paths of size 18, and Figure 21 shows all triples of non-intersecting lattice paths of size 4. On these figures, the extremities of the paths are indicated by circles; an additional  $E$  (resp.  $N$ ) step has been represented at the beginning (resp. end) of the middle and lower paths. The reason for this choice will appear clearly later.

From the general techniques developed in [21, 16] (and applied to the case of interest to us in [26]), we know that triples of non-intersecting lattice paths are enumerated by Baxter numbers. In the following, we exhibit a size-preserving bijection between these objects and Baxter TLTs.

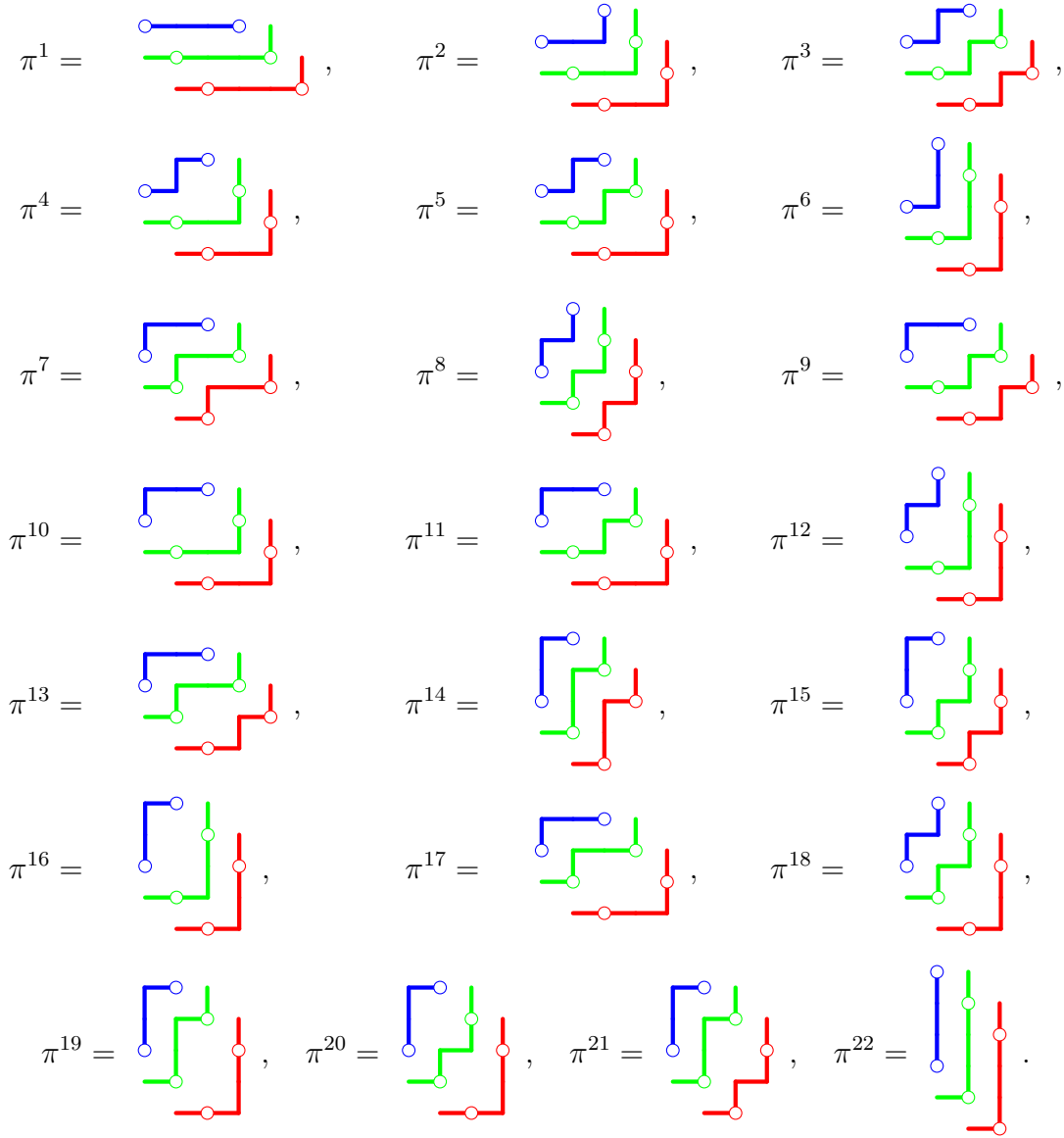


FIGURE 21. The 22 triples of non-intersecting paths of  $\mathcal{P}_4$ .

### 5.1. A bijection between binary trees and pairs of non-intersecting lattice paths.

The announced bijection actually extends a bijection between binary trees and pairs of non-intersecting lattice paths, which we describe below. In our context, a pair of non-intersecting lattice paths of size  $n$  is a pair of lattice paths with unitary  $N$  and  $E$  steps, which never meet, starting at  $(1, 0)$  and  $(0, 1)$  and ending at  $(n - i, i)$  and  $(n - i - 1, i + 1)$  for some  $i \in [0..(n - 1)]$  (thus each of the two paths has  $n - 1$  steps).

To any binary tree  $B$ , we associate a word  $w(B)$  on the alphabet  $\{L_\ell, L_r, E_\ell, E_r\}$  as follows. We complete  $B$  by leaves, *i.e.*, we compute the complete binary tree  $B_c$  whose

internal nodes form the tree  $B$ . We perform the depth first traversal of  $B_c$ , starting on the left. We start with an empty word  $w = \varepsilon$ . Whenever a left leaf (resp. right leaf, left internal edge, right internal edge) is first encountered, we append  $L_\ell$  (resp.  $L_r, E_\ell, E_r$ ) to the end of  $w$  (except for the first and the last leaves of  $B_c$ , in which case we do nothing). When the traversal of  $B_c$  is over, we set  $w(B) = w$ .

We define  $w_1(B)$  from  $w(B)$  by deleting the letters  $L_\ell$  and  $L_r$  and by replacing letters  $E_\ell$  (resp.  $E_r$ ) by  $N$  (resp.  $E$ ). Similarly, we define  $w_2(B)$  from  $w(B)$  by deleting the letters  $E_\ell$  and  $E_r$  and by replacing letters  $L_\ell$  (resp.  $L_r$ ) by  $E$  (resp.  $N$ ). Finally, we set  $\varphi(B) = (w_1(B), w_2(B))$ . Our notational convention is that the word  $w_1(B)$  (resp.  $w_2(B)$ ) designate the upper (resp. lower) path of the pair, starting at  $(0, 1)$  (resp.  $(1, 0)$ ).

Note that treating the first and last leaves of  $B_c$  like all others does not change much in the pair of words produced: it only results in replacing  $w_2(B)$  by  $E \cdot w_2(B) \cdot N$ . In figures, we usually indicate those additional steps, before and after the circles marking the extremities of the paths.

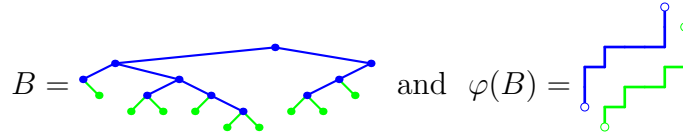


FIGURE 22. The bijection  $\varphi$ . On the left, a binary tree  $B$  is shown in blue, and the leaves added to obtain  $B_c$  are drawn in green. On the right, the two paths  $w_1(B)$  and  $w_2(B)$  that define  $\varphi(B)$  are shown respectively in blue and green.

In this figure, I would add the first and the last leaves of  $B_c$ , and the E and N step at the ends of the green path.

Figure 22 provides an example of this construction. For this particular tree  $B$ , we have  $w(B) = E_\ell E_\ell L_r E_r E_\ell L_\ell L_r E_r L_\ell E_r L_\ell L_r E_r E_\ell E_\ell L_\ell L_r L_r$ , so that  $w_1(B) = NNENEEENN$  and  $w_2(B) = NENEENENN$ .

**Proposition 39.**  $\varphi$  is a bijection between binary trees having  $n$  nodes and pairs of non-intersecting lattice paths of size  $n$ .

Notice that  $\varphi$  has already been defined in [14], where it is stated that it provides an alternative description of the bijection of [12] between binary trees and parallelogram polyominoes. Proposition 39 follows directly from this statement, which is however not proved in [14]. For this reason, we prefer to give here a proof of Proposition 39.

*Proof.* Denoting  $C_n = \frac{1}{n+1} \binom{2n}{n}$  the  $n$ -th Catalan number, we know that there are  $C_n$  binary trees with  $n$  nodes as well as  $C_n$  pairs of non-intersecting lattice paths of size  $n$  [21, 16]. Therefore, to prove that  $\varphi$  is a bijection as claimed, it is enough to prove that the image of  $\varphi$  is included in the set of pairs of non-intersecting lattice paths, and that  $\varphi$  is injective.

Let  $B$  be a binary tree with  $n$  nodes. We want to prove that  $\varphi(B)$  is a pair of non-intersecting lattice paths of size  $n$ . For this purpose, let us define the correspondence  $(\star)$

between the left (resp. right) internal edges and the right (resp. left) leaves of  $B_c$  (except the first and the last leaves) as follows: to any left (resp. right) internal edge whose lower node is  $x$ , associate the right (resp. left) leaf that is reached when following (in  $B_c$ ) only right (resp. left) edges from  $x$  until a right (resp. left) leaf is reached. A simple observation, which is however a key fact, is that this correspondence is a bijection. This is illustrated on Figure 23. For the green labels, change  $x$  to  $x^*$  and  $i$  to  $i^*$  for all  $i$ ?

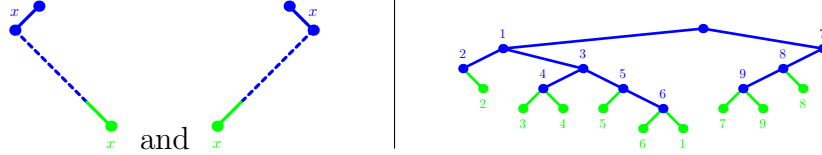


FIGURE 23. The correspondence  $(\star)$ : its definition (left) and an illustration with the example of Figure 22 (right). On the right, the correspondence is indicated by a labeling of the nodes by integers: the leaf labeled by  $i$  is in correspondence with the internal edge whose lower node is labeled by  $i$ .

Now let us denote by  $i \in [0..(n-1)]$  the number of  $N$  steps of  $w_1(B)$ . Since  $w_1(B)$  starts at  $(0, 1)$ , it ends at  $(n-i-1, i+1)$ . Because  $(\star)$  is a bijection,  $w_1(B)$  and  $w_2(B)$  have the same number of  $N$  (resp.  $E$ ) steps, so that  $w_2(B)$ , starting at  $(1, 0)$ , ends at  $(n-i, i)$ .

Next, we claim that  $w_1(B)$  is always strictly above  $w_2(B)$ . To prove this claim, let us consider the coordinates of the points visited by  $w_1(B)$ . They are of the form (number of right edges visited,  $1+$  number of left edges visited) when we consider all instants of the depth first traversal of  $B_c$ . Similarly, the coordinates of the points of  $w_2(B)$  are of the form ( $1+$  number of left leaves visited, number of right leaves visited) (always leaving aside the first and last leaves). So the claim will follow if we prove that at any instant of the traversal of  $B_c$ , if the number of left leaves visited (including the first one) is equal to the number of right edges visited, then the number of left edges visited is larger than or equal to the number of right leaves visited. This is easily proved using the correspondence  $(\star)$  between leaves and edges of  $B$ . Indeed, in the traversal of  $B$ , any left (resp. right) edge is visited before the corresponding right (resp. left) leaf.

It remains to prove that  $\varphi$  is injective. Consider  $B$  and  $B'$  two different binary trees with  $n$  nodes. Of course, the words  $w(B)$  and  $w(B')$  encoding the depth-first traversals of  $B_c$  and  $B'_c$  are different. We prove that  $w(B) \neq w(B')$  implies that  $\varphi(B) \neq \varphi(B')$ .

Consider the first time  $w(B)$  and  $w(B')$  differ:  $w(B)_j \neq w(B')_j$  while  $w(B)_k = w(B')_k$  for all  $k < j$ . The possible values for the pair of letters  $(w(B)_j, w(B')_j)$  (up to the order) are described in the following table, together with the subsequent difference between  $\varphi(B)$  and  $\varphi(B')$ . In this table, we denote by  $i_1$  (resp.  $i_2$ ) the number of letters  $E_r$  or  $E_\ell$  (resp.  $L_r$  or  $L_\ell$ ) among the first  $j$  letters of  $w(B)$ . Therefore, the letter  $w(B)_j$  corresponds either to  $w_1(B)_{i_1}$  or to  $w_2(B)_{i_2}$  (depending on whether  $w(B)_j \in \{E_r, E_\ell\}$  or  $w(B)_j \in \{L_r, L_\ell\}$ ).

$w(B)_j$	$w(B')_j$	Difference	Fact(s) used
$E_\ell$	$E_r$	$w_1(B)_{i_1} = N$ and $w_1(B')_{i_1} = E$	(obvious)
$E_\ell$	$L_\ell$	$w_1(B)_{i_1} = N$ and $w_1(B')_{i_1} = E$	(a)
$E_\ell$	$L_r$	$w_1(B)_{i_1} = N$ and $w_1(B')_{i_1} = E$	(a)
$E_r$	$L_r$	$w_2(B)_{i_2} = E$ and $w_2(B')_{i_2} = N$	(b)
$E_r$	$L_\ell$	In this case, $w(B)_{j-1} \neq w(B')_{j-1}$ , contradicting the minimality of $j$ .	(c) and (d)
$L_r$	$L_\ell$	$w_2(B)_{i_2} = N$ and $w_2(B')_{i_2} = E$	(obvious)

All these cases follow from the following facts:

- (a) When the traversal reaches a leaf, then the next edge to be discovered is a right edge.
- (b) When the traversal reaches an edge, then the next leaf to be discovered is a left leaf.
- (c) In any depth-first traversal word  $w(B)$ , any letter  $E_r$  follows a letter  $L_r$  or  $L_\ell$ .
- (d) In any depth-first traversal word  $w(B)$ , any letter  $L_\ell$  follows a letter  $E_r$  or  $E_\ell$ .  $\square$

5.2. **Extension to a bijection between  $\mathcal{T}_n$  and  $\mathcal{P}_n$ .** To any TLT  $T \in \mathcal{T}_n$ , we may associate a binary tree  $B(T)$  with  $n$  nodes, as explained in Section 2 (see also an example in Figure 24, left). We define  $\Phi_{\mathcal{P}}(T) = (w_{top}(T), w_{middle}(T), w_{bottom}(T))$  as follows:

- $w_{top}(T)$ , from  $(-1, 2)$  to  $(n - i - 2, i + 2)$ , is  $w_1(B(T))$ .
- $w_{middle}(T)$ , from  $(0, 1)$  to  $(n - i - 1, i + 1)$ , is  $w_2(B(T))$ .
- $w_{bottom}(T)$ , from  $(1, 0)$  to  $(n - i, i)$ , is the Southeast border of  $T$ , except the first and the last edge.

Figure 24 illustrates this construction. Note that the TLTs of Figures 24 and 5 (right) (p.8) differ only by their underlying Ferrers diagrams.

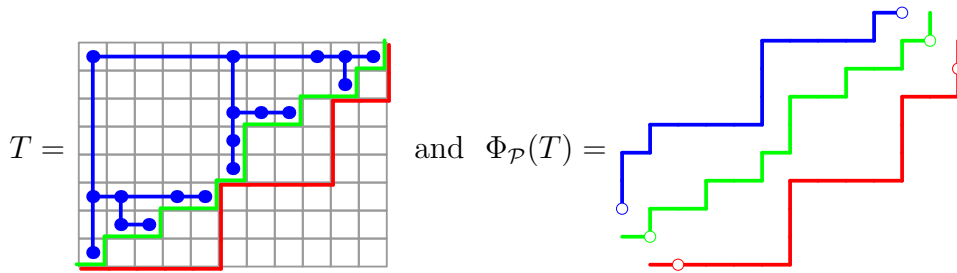


FIGURE 24. The bijection  $\Phi_{\mathcal{P}}$ .

Recall from Corollary 9 that any binary tree is the underlying tree of a unique rectangular Baxter TLT. This fact will be useful both for proving that  $\Phi_{\mathcal{P}}$  is well-defined and that it is a bijection between  $\mathcal{T}_n$  and  $\mathcal{P}_n$ .

**Lemma 40.**  $\Phi_{\mathcal{P}}$  is well-defined, i.e., for any  $T \in \mathcal{T}_n$ ,  $\Phi_{\mathcal{P}}(T)$  is a triple of non-intersecting lattice paths of size  $n$ .

*Proof.* From Proposition 39, we know that  $w_{top}(T)$  and  $w_{middle}(T)$  are a pair of non-intersecting lattice paths of size  $n$ . So the conclusion will follow if we prove that  $w_{middle}(T)$  and  $w_{bottom}(T)$  also form a pair of non-intersecting lattice paths of size  $n$ . This is an immediate consequence of the following claim (which we then prove):  $E \cdot w_{middle}(T) \cdot N$  can also be interpreted as the Southeast border of the thinnest Ferrers diagram containing all the points of  $T$  (see Figure 24, left).

From Corollary 9, we know that there is a unique TLT  $T'$  of rectangular shape avoiding the patterns  $\begin{smallmatrix} \blacksquare & \blacksquare \\ \blacksquare & \blacksquare \end{smallmatrix}$  and  $\begin{smallmatrix} \blacksquare & \blacksquare \\ \blacksquare & \blacksquare \end{smallmatrix}$  whose underlying binary tree is  $B(T)$ . Moreover, the proof of Corollary 9 provides a description of  $T'$ . By uniqueness, the points of  $T$  and  $T'$  are located in the same cells. Consequently, it is enough to show that the Southeast border of the thinnest Ferrers diagram containing all the points of  $T'$  is  $E \cdot w_{middle}(T) \cdot N$ .

From the description of  $T'$  in the proof of Corollary 9, we see that the Southeast border of the thinnest Ferrers diagram containing all the points of  $T'$  is nothing but the reading of the leaves of  $B(T')_c$  in the depth-first traversal of  $B(T')_c$  (with the encoding  $E$  for a left leaf and  $N$  for a right leaf). By definition,  $E \cdot w_{middle}(T) \cdot N$  describes the leaves of  $B(T)_c$  that are visited in the depth-first traversal of  $B(T)_c$ . Because  $B(T) = B(T')$ , the conclusion follows.  $\square$

**Theorem 41.** *For any  $n$ ,  $\Phi_{\mathcal{P}}$  is a bijection between  $\mathcal{T}_n$  and  $\mathcal{P}_n$ .*

*Proof.* Lemma 40 ensures that the image of  $\mathcal{T}_n$  by  $\Phi_{\mathcal{P}}$  is included in  $\mathcal{P}_n$ . In addition, from Theorem 30 and [17, for instance], the cardinality of  $\mathcal{T}_n$  is  $Bax_n$ , and the same holds for  $\mathcal{P}_n$  [26]. So it is enough to prove that  $\Phi_{\mathcal{P}}$  is a bijection. By Corollary 9, a Baxter TLT  $T \in \mathcal{T}_n$  is uniquely characterized by the pair  $(B(T), w_{bottom}(T))$ . Moreover, by Proposition 39, we may associate with  $B(T)$  the pair  $(w_{top}(T), w_{middle}(T))$ , and this correspondence is bijective. Therefore, the correspondence between  $T \in \mathcal{T}_n$  and  $(w_{top}(T), w_{middle}(T), w_{bottom}(T)) \in \mathcal{P}_n$  is a bijection.  $\square$

**5.3. Refined enumeration using the Lindström-Gessel-Viennot lemma.** We derive easily from the Lindström-Gessel-Viennot lemma [21, 16] a refined enumeration of triples of non-intersecting paths, according to the parameters shown on Figure 25. This yields a refined enumeration of Baxter TLTs via  $\Phi_{\mathcal{P}}$ , and subsequently of PFPs and permutations avoiding  $3 - 14 - 2$  and  $3 - 41 - 2$  via  $\Phi_{\mathcal{F}}$  and  $\Phi_{\mathcal{B}}$ .

**Lemma 42.** *The number of triples of non-intersecting paths of size  $n$  such that each path has  $k$   $E$  steps and  $n - 1 - k$   $N$  steps, the upper path starts with  $r - 1$   $N$  steps followed by an  $E$  step, and ends with  $p - 1$   $E$  steps preceded by a  $N$  step, and the lower path starts with  $s - 1$   $E$  steps followed by a  $N$  step, and ends with  $q - 1$   $N$  steps preceded by an  $E$  step (see Figure 25) is given by the determinant:*

$$LGV(n, k, r, p, s, q) = \begin{vmatrix} \binom{n-1-r-p}{k-p} & \binom{n-1-p}{k-p} & \binom{n-1-s-p}{k-s-p} \\ \binom{n-1-r}{k} & \binom{n-1}{k} & \binom{n-1-s}{k-s} \\ \binom{n-1-r-q}{k} & \binom{n-1-q}{k} & \binom{n-1-s-q}{k-s} \end{vmatrix}.$$

*Proof.* This is a simple application of the results of [21, 16].  $\square$



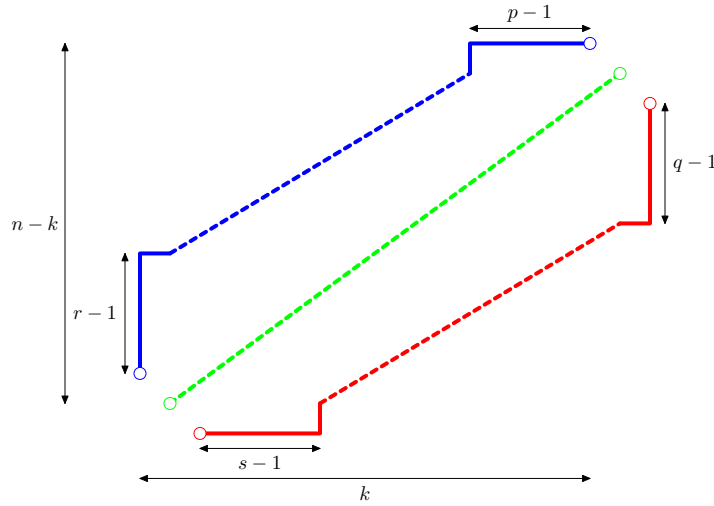


FIGURE 25. Parameters for the refined enumeration of triples of non-intersecting paths in Lemma 42.

**Corollary 43.** *The determinant  $LGV(n, k, r, p, s, q)$  also counts the number of Baxter TLTs of size  $n$ , with  $k + 1$  columns,  $r$  points in the first column, and  $p - 1$  columns to the right of the rightmost column containing at least two points<sup>4</sup>, and such that the Southeast border of the Ferrers diagram of the TLT starts with  $s$  horizontal steps and ends with  $q$  vertical steps.*

For example, the TLT  $T$  of Figure 24 has parameters  $n = 18$ ,  $k = 10$ ,  $r = 3$ ,  $p = 2$ ,  $s = 5$ , and  $q = 2$ .

*Proof.* It can be easily checked that all parameters in Lemma 42 are translated on TLTs through  $\Phi_{\mathcal{P}}$  as stated in Corollary 43. For instance, the upper path of  $\Phi_{\mathcal{P}}(T)$  ends with exactly  $p - 1$   $E$  steps if and only if exactly the last  $p - 1$  internal edges of  $B(T)$  in the depth-first search are right edges, which translates into exactly the  $p - 1$  rightmost columns of  $T$  containing a single point.  $\square$

**Corollary 44.** *The number of PFPs of size  $n$ , in a bounding rectangle of height  $n - k$  and width  $k + 1$ , with  $r$  tiles whose left edge is supported by the left edge of the bounding rectangle, and such that the rightmost vertical line that supports the left edge of at least two tiles is at distance  $p$  from the right edge of the bounding rectangle is  $\sum_{q,s} LGV(n, k, r, p, s, q)$ .*

*The number of permutations of size  $n$ , avoiding  $3 - 14 - 2$  and  $3 - 41 - 2$ , with  $k$  ascents and  $r$  left-to-right minima is  $\sum_{p,q,s} LGV(n, k, r, p, s, q)$ .*

*Proof.* It is enough to check that the parameters  $n$ ,  $k$ ,  $r$  and  $p$  in Corollary 43 are translated on PFPs and permutations avoiding  $3 - 14 - 2$  and  $3 - 41 - 2$  via  $\Phi_{\mathcal{F}}$  and  $\Phi_{\mathcal{B}}$  as expressed in the statement of Corollary 44.

<sup>4</sup>Necessarily, each of these  $p - 1$  columns contains a single point.

Because  $\Phi_{\mathcal{F}}$  maps  $\mathcal{T}_{(n-k,k+1)}$  to  $\mathcal{F}_{(n-k,k+1)}$ , we are only left with the interpretation of the parameters  $r$  and  $p$  on PFPs. They follow easily from the description of  $\Phi_{\mathcal{F}}$ , since any point  $x$  of  $T$  is associated with a tile whose top-left corner is the cell containing  $x$ .

Consider now  $T \in \mathcal{T}_n$  and  $\sigma = \Phi_{\mathcal{B}}(T) \in \mathcal{B}_n$ . From Corollary 35, the number of ascents in  $\sigma$  is the number of column-extremal points in  $T$ . Since there is one such point in each column except the first, this solves the case of parameter  $k$ . From Corollary 37, there is one left-to-right minimum for each point in the first column, proving the statement for the parameter  $r$ .  $\square$

## 6. SPECIALIZATIONS OF THE BIJECTIONS

Using the underlying tree structure of TLTs, we define a subfamily (denoted  $\hat{\mathcal{T}}$ ) of Baxter TLTs whose nice combinatorial properties are explained in this section.

For each of the studied bijections,  $\Phi_{\mathcal{P}}$ ,  $\Phi_{\mathcal{F}}$  and  $\Phi_{\mathcal{B}}$ , we consider its restriction to the domain  $\hat{\mathcal{T}}$ . These restrictions, denoted  $\hat{\Phi}_{\mathcal{P}}$ ,  $\hat{\Phi}_{\mathcal{F}}$  and  $\hat{\Phi}_{\mathcal{B}}$ , provide bijections between  $\hat{\mathcal{T}}_n$  and subclasses of  $\mathcal{P}_n$ ,  $\mathcal{F}_n$  and  $\mathcal{B}_n$ , which we denote  $\hat{\mathcal{P}}_n$ ,  $\hat{\mathcal{F}}_n$  and  $\hat{\mathcal{B}}_n$ . As we shall see, the family  $\hat{\mathcal{P}}_n$  is well-known, giving easy access to the enumeration of these restricted families, the definition of  $\hat{\mathcal{F}}_n$  involves a new type of constraint in floorplans, and the permutations of  $\hat{\mathcal{B}}_n$  are natural combinatorial objects. In particular, the enumeration of the permutations of  $\hat{\mathcal{B}}_n$  triggers some intriguing enumerative problems, which we discuss at the end of this section.

For now, we define the subfamily  $\hat{\mathcal{T}}$  and state a lemma which is essential to analyze the restrictions of our bijections.

**Definition 45.** *A complete Baxter TLT is a Baxter TLT whose underlying tree is a complete binary tree.*

*An almost complete Baxter TLT of size  $n$  is a Baxter TLT of size  $n$  whose underlying tree is almost complete: namely, it is complete binary tree from which the following have been removed:*

- *the leaf  $\ell$  that is reached from the root when following only left edges, if  $n$  is even;*
- *$\ell$  and the leaf  $r$  that is reached from the root when following only right edges, if  $n$  is odd;*

*We denote by  $\hat{\mathcal{T}}_n$  the set of almost complete Baxter TLT of size  $n$ .*

Figures 26 and 27 show some examples.

**Lemma 46.** *Let  $T$  be a Baxter TLT, and define its leaves as its points which correspond to leaves of the underlying tree of  $T$ . The followings are equivalent:*

- *$T$  is a complete Baxter TLT;*
- *the leaves of  $T$  form a staircase shape, i.e., they are located on the Southwest-Northeast diagonal which starts at the bottommost point of the first column of  $T$ , and occupy every cell of this diagonal.*

*Proof.* We note that a complete Baxter TLT is necessarily of odd size. We also observe that a TLT satisfying the second condition above is also necessarily of odd size: indeed,

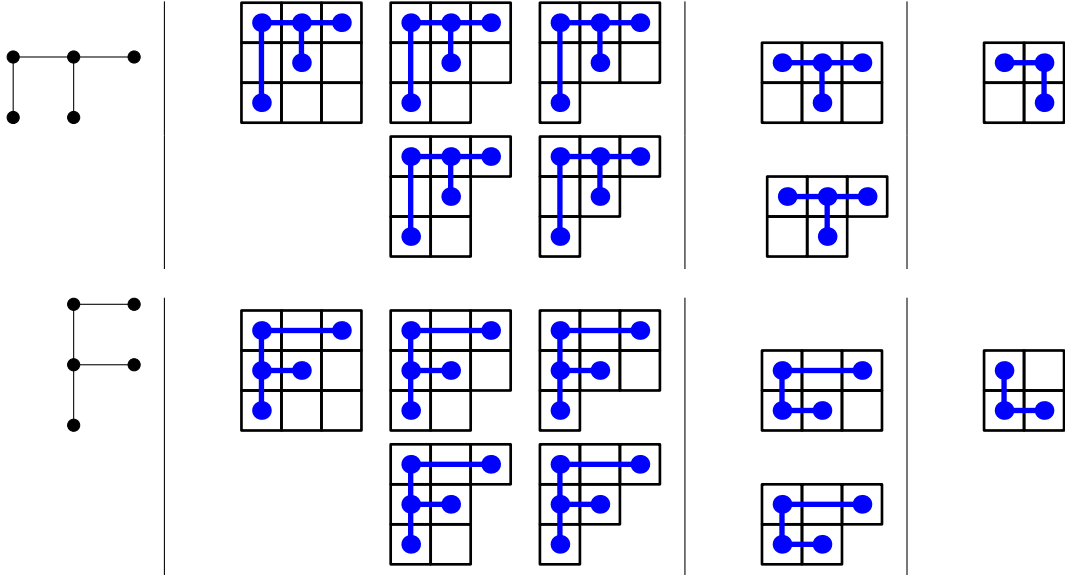
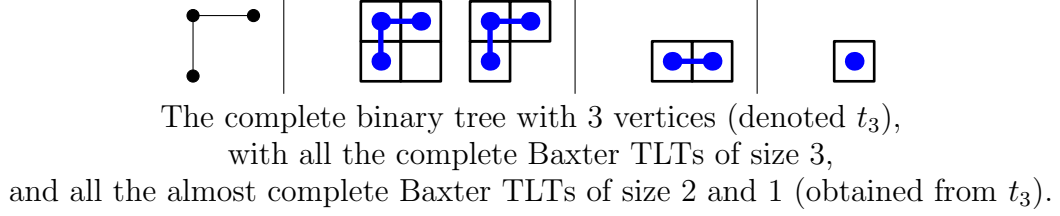


FIGURE 26. Small complete and almost complete Baxter TLTs. (For consistency with TLTs, the roots of binary trees are drawn in the top left.)

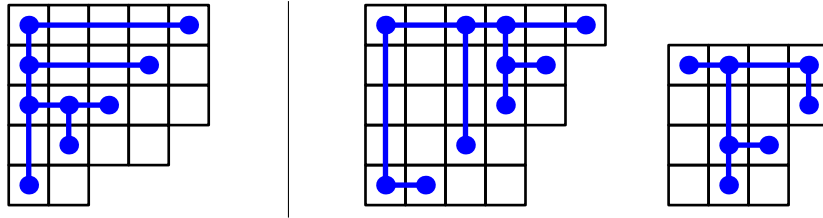


FIGURE 27. Left: A complete Baxter TLT of size 9. Right: Two almost complete Baxter TLTs, of respective size 10 and 7.

recalling that there are no empty rows nor columns in TLTs, it is forced to have  $n$  rows and  $n$  columns for some  $n$ , and therefore  $2n - 1$  points.

We prove the claimed statement for all Baxter TLTs of size  $2n + 1$  by induction on  $n$ . The base case  $n = 0$  is obvious.

Let  $T$  be a Baxter TLT of size  $2n + 1$  for  $n > 0$ . Consider the bi-partition  $(L, R)$  of the non-root points of  $T$  where  $L$  (resp.  $R$ ) contains all points of  $T$  in the left (resp. right) subtree pending from the root of the underlying tree of  $T$ . From Proposition 8 and Corollary 10,  $T$  can be decomposed into 4 blocks as  $\frac{A|D}{B|C}$ , with  $A$  containing only the root of  $T$ ,  $B$  (resp.  $D$ ) containing all points of  $L$  (resp.  $R$ ), and  $C$  containing no points. We recall that a binary tree is complete if and only if the left and right subtrees pending from its root are also complete binary trees.

It follows that, if  $T$  is a complete Baxter TLT, then  $B$  and  $D$  are also complete Baxter TLTs. They are smaller than  $T$ , and by induction have their leaves which form a staircase shape. This consequently also holds for the leaves of  $T$ , which form a staircase shape obtained from the concatenation of those of  $B$  and  $D$ . Conversely, if the leaves of  $T$  form a staircase shape, then it also holds for those of  $B$  and  $D$ , which are therefore complete Baxter TLTs, implying that  $T$  also is a complete Baxter TLT.  $\square$

### 6.1. Restriction on lattice paths.

**Proposition 47.** *Let  $\hat{\mathcal{P}}_n$  be the set of pairs of Dyck paths with  $n$  steps, if  $n$  is even (resp. with  $n + 1$  and  $n - 1$  steps respectively, if  $n$  is odd). Define  $\bar{\Phi}_{\mathcal{P}}$  as follows:*

- *if  $n$  is even, then for all  $T \in \hat{\mathcal{T}}_n$ , writing  $\hat{\Phi}_{\mathcal{P}}(T) = (w_{top}, w_{middle}, w_{bottom})$ , we set  $\bar{\Phi}_{\mathcal{P}}(T) = (N \cdot w_{top}, w_{bottom} \cdot N)$ ;*
- *if  $n$  is odd, then for all  $T \in \hat{\mathcal{T}}_n$ , writing  $\hat{\Phi}_{\mathcal{P}}(T) = (w_{top}, w_{middle}, w_{bottom})$ , we set  $\bar{\Phi}_{\mathcal{P}}(T) = (N \cdot w_{top} \cdot E, w_{bottom})$ .*

*Then, it holds that  $\bar{\Phi}_{\mathcal{P}}$  is a bijection between  $\hat{\mathcal{T}}_n$  and  $\hat{\mathcal{P}}_n$ .*

*Proof.* To prove this statement, we must keep in mind the interpretation of the three paths of  $\hat{\Phi}_{\mathcal{P}}(T) = (w_{top}, w_{middle}, w_{bottom})$  for  $T \in \hat{\mathcal{T}}_n$  explained in the proof of Lemma 40. In particular, the following holds.

- $w_{top}$  encodes the underlying tree structure of  $T$ . In the present case where  $T \in \hat{\mathcal{T}}_n$ , this implies that  $N \cdot w_{top}$  when  $n$  is even and  $N \cdot w_{top} \cdot E$  when  $n$  is odd encodes the complete binary tree from which  $T$  was built (hence, in particular, is a generic Dyck path).
- $w_{middle}$  has been obtained from the path which follows the leaves of  $T$  by removing the first and the last steps. For  $T \in \hat{\mathcal{T}}_n$ , Lemma 46 implies that  $w_{middle}$  is an alternation of  $N$  and  $E$  steps starting with an  $E$ .
- $w_{bottom}$  is the Southeast border of  $T$  from which the first and last steps have been removed. Since  $w_{bottom}$  is a path located to the Southeast of  $w_{middle}$ , and given the very specific form of  $w_{middle}$  in our case, this implies that  $w_{bottom} \cdot N$  if  $n$  is even (resp.  $w_{bottom}$  if  $n$  is odd) is the symmetric of a generic Dyck path w.r.t. the main diagonal.

Summing up, this shows that pairs  $(d_t, d_b)$  of Dyck paths in  $\hat{\mathcal{P}}_n$  are (up to removing initial and/or final steps as described above) in bijection with triples of non-intersecting

paths of size  $n$  whose middle path is an alternation of single  $N$  and  $E$  steps starting with  $E$ , which are themselves in bijection with  $\hat{\mathcal{T}}_n$  by Lemma 46, thus concluding the proof.  $\square$

Figure 28 shows the triples of non-intersecting paths and the corresponding pairs of Dyck paths of the two almost complete Baxter TLTs of even and odd size given in Figure 27.

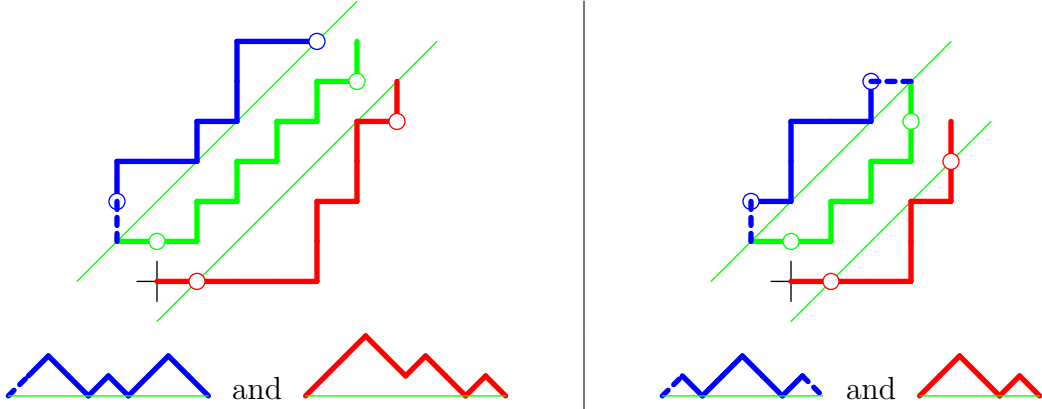


FIGURE 28. Two triples of non-intersecting paths and the corresponding pairs of Dyck paths.

Voir si c'est opportun de mettre certains pas en pointillé (et le faire de manière cohérente).

Proposition 47 has an immediate enumerative consequence:

**Corollary 48.** *For any  $n$ , the cardinality of  $\hat{\mathcal{T}}_{2n}$  is  $C_n^2$ , and the one of  $\hat{\mathcal{T}}_{2n+1}$  is  $C_n \cdot C_{n+1}$ , where  $C_n = \frac{1}{n+1} \binom{2n}{n}$  is the  $n$ -th Catalan number.*

**6.2. Restriction on floorplans.** In the characterization of the image of  $\hat{\mathcal{T}}_n$  under the bijection  $\Phi_{\mathcal{F}}$  between Baxter TLTs and packed floorplans, we are led to defining a new class of floorplans with constraints along the Southwest-Northeast diagonal.

Recall from Section 3 that floorplans are rectangular partitions of a rectangle such that every pair of segments with non-empty intersection forms a  $T$ -junction.

**Definition 49.** *An alternating floorplan of size  $n$  is a partition of a rectangle  $R$  of width  $\lceil \frac{n+1}{2} \rceil$  and height  $\lfloor \frac{n+1}{2} \rfloor$  into  $n$  rectangular tiles whose sides have integer lengths such that the path from the Southwest corner to the Northeast corner of  $R$  which moves alternately one unit step East and one unit step North (starting with East) is included in the boundaries of partitioning rectangles of  $F$ . We call this path the alternating path of  $F$ .*

We denote by  $\hat{\mathcal{F}}_n$  the set of alternating floorplans of size  $n$ .

Figure 29 (left) shows an example of an alternating floorplan.

We will show that  $\hat{\mathcal{F}}_n$  is indeed included in the family  $\mathcal{F}_n$  of packed floorplans. To this end, we first state an important property of the alternating paths of alternating floorplans.

**Lemma 50.** *In any alternating floorplan  $F$ , every tile has either its bottomright corner or its topleft corner on the alternating path of  $F$ .*

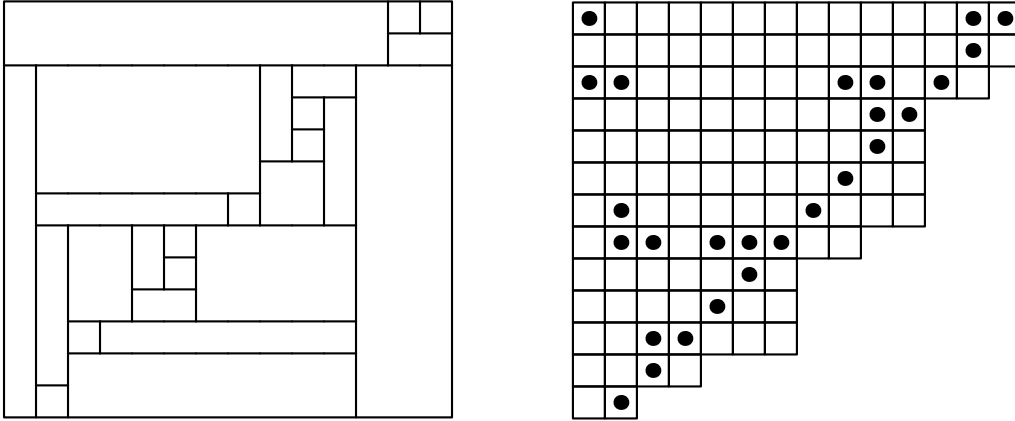


FIGURE 29. Left: An alternating floorplan  $F$  of size 26. Right: The almost complete Baxter TLT  $T$  of size 26 such that  $\hat{\Phi}_{\mathcal{F}}(T) = F$ .

*Proof.* Let us denote by  $n$  the size of  $F$ . By definition, the alternating path of  $F$  contains  $\lceil n/2 \rceil$  factors  $EN$  and  $\lfloor n/2 \rfloor$  factors  $NE$ , each corresponding to a bottomright corner or a topleft corner of a tile of  $F$ , respectively. This gives a total of  $n$  tiles, necessarily all distinct, and therefore all tiles of  $F$  have their bottomright or topleft corner on the alternating path as claimed.  $\square$

When a tile  $t$  of an alternating floorplan  $F$  has its topleft (resp. bottomright) corner on the alternating path of  $F$ , we say that  $t$  is *below* (resp. *above*) the alternating path of  $F$ .

**Lemma 51.** *Every alternating floorplan is a packed floorplan.*

*Proof.* Let  $F$  be an alternating floorplan of size  $n$ . To prove that  $F$  is a packed floorplan, comparing with Definition 11, we only need to check that  $F$  avoids the pattern  $\begin{smallmatrix} \lrcorner \\ \lrcorner \end{smallmatrix}$ .

Assume that two tiles  $t$  and  $t'$  of  $F$  form a  $\begin{smallmatrix} \lrcorner \\ \lrcorner \end{smallmatrix}$  pattern. Using Lemma 50, we distinguish three cases (w.l.o.g. up to exchanging  $t$  and  $t'$ ): either  $t$  is above the alternating path and  $t'$  is below it, or  $t$  and  $t'$  are both above the alternating path, or they are both below. In the first case, because of the alternating path condition, the bottomright corner of  $t$  is forced to sit either above and to the right, or below and to the left, of the topleft corner of  $t'$ . But this is impossible when  $t$  and  $t'$  form a pattern  $\begin{smallmatrix} \lrcorner \\ \lrcorner \end{smallmatrix}$ . In the second case, the bottomright corners of  $t$  and  $t'$  are forced to sit as  $\begin{smallmatrix} \lrcorner \\ \lrcorner \end{smallmatrix}$  by the alternating path condition, but as  $\begin{smallmatrix} \lrcorner \\ \lrcorner \end{smallmatrix}$  by the occurrence of  $\begin{smallmatrix} \lrcorner \\ \lrcorner \end{smallmatrix}$ , also yielding a contradiction. The third case is similar, considering the topleft corners of  $t$  and  $t'$ . This concludes the proof that  $F$  avoids  $\begin{smallmatrix} \lrcorner \\ \lrcorner \end{smallmatrix}$ , hence is a packed floorplan.  $\square$

**Proposition 52.**  $\hat{\Phi}_{\mathcal{F}}$  is a bijection between  $\hat{\mathcal{T}}_n$  and  $\hat{\mathcal{F}}_n$ .

*Proof.* Consider an alternating floorplan  $F \in \hat{\mathcal{F}}_n$  and its preimage  $T$  under  $\Phi_{\mathcal{F}}$ . We know that  $T$  is a Baxter TLT. To prove that it is almost complete, we use Lemma 50 to ensure that  $T$  as  $\lfloor n/2 \rfloor$  points on the main diagonal (shifted by one unit to the right): namely, those corresponding to the topleft corners of the tiles below the alternating path of  $F$ . Then, Lemma 46 ensures that  $T$  is an almost complete Baxter TLT.

Conversely, for an almost complete Baxter TLT  $T$ , we show that  $\Phi_{\mathcal{F}}(T)$  is an alternating floorplan by ensuring that it contains a valid alternating path. Lemma 46 forces the placement of the topleft corners of some tiles of  $F$ , namely, those whose topleft corner is a leaf of  $T$ . As a consequence, the path  $E(NE)^{\lfloor n/2 \rfloor} N^\delta$  is supported by the sides of the tiles of  $F$ , for  $\delta = 0$  if  $n$  is even and  $\delta = 1$  if  $n$  is odd. More precisely, the first  $E$  step is supported by the bottom edge of the bounding rectangle of  $F$  (hence by its bottomleftmost tile), each  $NE$  factor surrounds the topleft corner of a tile corresponding to a leaf of  $T$ , and, in case  $n$  is odd, the final  $N$  step is supported by the right edge of the bounding rectangle of  $F$  (hence by its toprightmost tile).  $\square$

Figure 29 (right) shows an example of an almost complete Baxter TLT which is in bijection by  $\hat{\Phi}_{\mathcal{F}}$  with the alternating floorplan on the left of this figure.

**6.3. Restriction on permutations.** We recall that a permutation  $\sigma$  is *alternating* if the comparisons between consecutive elements alternate between ascents and descents, that is to say if  $\sigma(1) > \sigma(2) < \sigma(3) > \sigma(4) < \dots$  or  $\sigma(1) < \sigma(2) > \sigma(3) < \sigma(4) > \dots$ . Alternating permutations arise naturally when studying the restriction of our bijection  $\Phi_{\mathcal{B}}$  to  $\hat{\mathcal{T}}_n$ .

**Proposition 53.** *Let  $\hat{\mathcal{B}}_n$  be the set of permutations in  $\mathcal{B}_n$  that are alternating and start with an ascent.  $\hat{\Phi}_{\mathcal{B}}$  is a bijection between  $\hat{\mathcal{T}}_n$  and  $\hat{\mathcal{B}}_n$ .*

*Proof.* We first prove that the image of  $\hat{\mathcal{T}}_n$  by  $\hat{\Phi}_{\mathcal{B}}$  is included in  $\hat{\mathcal{B}}_n$ . So, consider  $T \in \hat{\mathcal{T}}_n$  and its image  $\sigma = \hat{\Phi}_{\mathcal{B}}(T)$ . We know that  $\sigma$  is in  $\mathcal{B}_n$ , and want to prove that  $\sigma$  is alternating starting with an ascent.

By construction,  $\sigma$  is the sequence of iso-labels read along the Southeast border of  $T$ . Recalling the rule for propagation of iso-labels (and in particular, the first item in Subsection 4.1), and the placement of the leaves of  $T$  (see Lemma 46), it follows that  $\sigma$  is also read on the path “inside”  $T$  along the boundary determined by the leaves. More precisely, we mean that  $\sigma$  is obtained by reading the iso-labels of the following cells of  $T$ , in this order: the bottommost cell of the first column, then its right neighbor (which is the first leaf), then the cell above it, then its right neighbor (which is the second leaf), and all cells subsequently met by moving alternately one cell to the top and one cell to the right, until the rightmost cell of the top row is reached. See Figure 30 for an illustration of this fact.

So,  $\sigma$  alternates between reading iso-labels of leaves and iso-labels of pointed or empty cells corresponding to internal nodes. The two leaves surrounding a pointed or empty cell with iso-label  $x$  have larger iso-labels, because the pointed cell of  $T$  carrying the iso-label  $x$  is an ancestor of both leaves. So  $\sigma$  is alternating. Moreover,  $\sigma$  starts with an ascent

because the first leaf is the second cell whose iso-label is read when building  $\sigma$  (the first cell read carrying as above the iso-label of an ancestor of this first leaf).

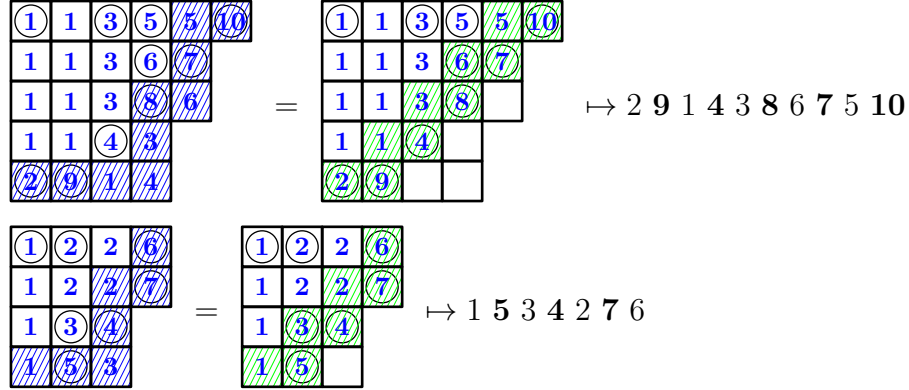


FIGURE 30. The two almost complete Baxter TLTs of Figure 27 with their iso-labeling, and the corresponding permutations. (The bold elements in permutations correspond to the leaves in the TLTs.)

Conversely, let  $\sigma \in \hat{\mathcal{B}}_n$ , and let  $T = \hat{\Phi}_B^{-1}(\sigma)$ .  $T$  is a Baxter TLT, and we want to prove that  $T$  is almost-complete. To this end, using Lemma 46, it is enough to prove that the leafs of  $T$  occupy all cells on the main diagonal starting at the second cell of the bottom row of  $T$  (which we refer to as *staircase shape*). To do so, our first step is to show that the points of  $T$  with iso-labels  $\sigma(2i)$  (for  $1 \leq i \leq \lfloor n/2 \rfloor$ ) are all leafs of  $T$ .

For any  $1 \leq i \leq \lfloor n/2 \rfloor$ , it holds that  $\sigma(2i-1) < \sigma(2i) > \sigma(2i+1)$  by the alternating condition (the second inequality being undefined in the case  $n$  is even and  $i = n/2$ ). Denote by  $\ell$  the point of  $T$  with iso-label  $\sigma(2i)$ . By Proposition 34 and Corollary 35, and according to Definition 33,  $\sigma(2i-1) < \sigma(2i) > \sigma(2i+1)$  implies that  $\ell$  is both column-extremal and row-extremal (except for the case  $n$  is even and  $i = n/2$ , in which case  $\ell$  is column-extremal and is the rightmost point in the first row). In particular, such points  $\ell$  are leafs of  $T$ .

Our next step is to show that these leafs form a staircase shape. We start by noticing that for any point  $c$  of  $T$  which is both column-extremal and row-extremal, all cells of  $T$  below and to the right of  $c$  must be empty. Indeed, assuming that a cell  $c'$  below and to the right of  $c$  were pointed, and considering w.l.o.g.  $c'$  topmost and leftmost among such cells,  $c$ ,  $c'$  and the parent of  $c'$  would form a pattern  $\begin{smallmatrix} \blacksquare & \blacksquare \\ \blacksquare & \blacksquare \end{smallmatrix}$  or  $\begin{smallmatrix} \blacksquare & \blacksquare \\ \blacksquare & \blacksquare \end{smallmatrix}$ .

Therefore, all pointed cells of  $T$  with iso-label  $\sigma(2i)$  for  $1 \leq i \leq \lfloor n/2 \rfloor$  must be in different columns and in different rows (by “extremality”). Moreover, considering these points from left to right gives a sequence of points which have increasing  $y$ -coordinates (since they have no point below and to their right).

As a consequence, the number of columns of  $T$  is at least  $1 + \lfloor n/2 \rfloor$ , the 1 accounting for the first column, and  $\lfloor n/2 \rfloor$  accounting for the column-extremal points  $\sigma(2i)$  for all  $i \in [1; \lfloor n/2 \rfloor]$ . Similarly, the number of rows must be at least  $\lfloor n/2 \rfloor + 1$  if  $n$  is odd (resp.



$\lfloor n/2 \rfloor$  if  $n$  is even, the point with iso-label  $\sigma(n)$  not being row-extremal in this case), yielding a total of at least  $n + 1$  rows and columns in total (both in the even and in the odd case). Since  $T \in \hat{\mathcal{T}}_n$ , we know that  $T$  has *exactly*  $n + 1$  rows and columns in total, implying that all the columns (except the leftmost) and all the rows (except the topmost when  $n$  is odd) are occupied by leaves of  $T$ , so that the leaves of  $T$  must form a staircase shape. Lemma 46 then concludes the proof.  $\square$

From Proposition 53 and Corollary 48, we immediately deduce the enumeration of  $\hat{\mathcal{B}}_n$ .

**Corollary 54.** *For any  $n$ , there are  $C_n^2$  (resp.  $C_n \cdot C_{n+1}$ ) permutations of size  $2n$  (resp.  $2n + 1$ ) which avoid the patterns  $3 - 14 - 2$  and  $3 - 41 - 2$  and are alternating starting with an ascent.*

**6.4. Enumerative problems opened the enumeration of alternating twisted Baxter permutations.** Corollary 54 provides an enumeration result which we have not been able to find in the literature. Our proof is bijective, and obtained as the result of composing two bijections: one between  $\hat{\mathcal{B}}_n$  and  $\hat{\mathcal{T}}_n$  and the other one between  $\hat{\mathcal{T}}_n$  and  $\hat{\mathcal{P}}_n$ . While this shows that TLT can be useful to prove meaningful results on other combinatorial objects, this also raises the question of whether  $\hat{\mathcal{B}}_n$  could be enumerated directly, without appealing to TLTs. It is not hard to observe that, for any permutation  $\sigma$  of  $\hat{\mathcal{B}}_n$ , its pattern  $\sigma_{\text{odd}}$  (resp.  $\sigma_{\text{even}}$ ) corresponding to the odd (resp. even) positions in  $[1, n]$  is a permutation avoiding 312 (resp. 231) as classical patterns. And it is well-known that the families  $Av(312)$  and  $Av(231)$  are enumerated by the Catalan numbers. Therefore, considering also the enumeration obtained in Corollary 54, it is tempting to conjecture that the map  $\sigma \mapsto (\sigma_{\text{odd}}, \sigma_{\text{even}})$  is a bijection between  $\hat{\mathcal{B}}_n$  and  $Av_{\lfloor n/2 \rfloor}(312) \times Av_{\lfloor n/2 \rfloor}(231)$ . We leave this question open.

In addition, we wish to point out that the permutations appearing in Corollary 54 are enumerated like the alternating Baxter permutations (*i.e.*, alternating permutations that avoid the patterns  $2 - 41 - 3$  and  $3 - 14 - 2$ ). Indeed, in [11], the authors give a bijective proof that the number of alternating Baxter permutations of size  $2n$  (resp.  $2n + 1$ ) is  $C_n^2$  (resp.  $C_n \cdot C_{n+1}$ ). Another combinatorial proof using triples of non-intersecting paths is given in [14].

Another important observation is that, unlike Baxter permutations, the permutations that avoid  $3 - 14 - 2$  and  $3 - 41 - 2$  are not stable under the reverse symmetry, nor under the complement symmetry. Therefore, Corollary 54 does not solve the enumeration of alternating permutations avoiding  $3 - 14 - 2$  and  $3 - 41 - 2$  and starting with a *descent*, whereas the results of [11, 14] do solve the analogous problem for Baxter permutations.

In view of these two very similar enumeration results, it is natural to look for a (hopefully simple) bijection between alternating Baxter permutations and alternating (inverses of) twisted Baxter permutations starting with an ascent. We leave this problem open, but point out one possible direction for finding such a bijection. In [15], the authors describe several bijections between families of Baxter objects, and in particular a bijection  $\Theta_1$  between Baxter permutations and pairs of twin binary trees, and a bijection  $\Theta_2$  between pairs of twin binary trees and *rectangulations*. These objects are exactly our packed floorplans, up to a rotation of  $90^\circ$ . The restriction of  $\Theta_1$  to alternating Baxter permutations provides a

bijection with pairs of twin binary trees with additional restrictions. A first task would be to examine how these restrictions are translated on the rectangulations (or packed floorplans) *via*  $\Theta_2$ , and then on the Baxter TLTs *via*  $\Phi_{\mathcal{F}}^{-1}$ . These restricted Baxter TLTs are equinumerous with the almost complete Baxter TLTs. It is actually possible that they are *exactly* the almost complete Baxter TLTs. If it is not the case, a second task would be to identify a bijection  $\Lambda$  between these two families of TLTs. A bijection between alternating Baxter permutations and alternating (inverses of) twisted Baxter permutations starting with an ascent would then be the composition  $\hat{\Phi}_{\mathcal{B}} \circ \Lambda \circ \Phi_{\mathcal{F}}^{-1} \circ \Theta_2 \circ \Theta_1$ . Describing this bijection directly would be the third task in this search of a *simple* bijection.

#### APPENDIX: SIZE-PRESERVING BIJECTION BETWEEN PFPs AND MOSAIC FLOORPLANS

Mosaic floorplans were defined as follows by Hong *et.al.* [18].

In a rectangular partition of a rectangle, a *segment* is a straight line, not included in the boundary of the partitioned rectangle, that is the union of some rectangle sides, and is maximal for this property. Let us call *floorplans* the rectangular partitions of a rectangle such that every pair of segments with non-empty intersection forms a T-junction (defined on p. 9). Two floorplans are said *R*-equivalent if one can pass from one to the other by sliding the segments to adjust the sizes of the rectangles. A *mosaic floorplan* is defined as an equivalence class of floorplans under *R*.

In [1], the authors describe a bijection between mosaic floorplans and Baxter permutations, *i.e.*, permutations avoiding the patterns  $2-41-3$  and  $3-14-2$  (see the definition of dashed patterns in Section 4). This implies that mosaic floorplans are enumerated by Baxter numbers. From Theorems 14 and 30, and since twisted Baxter permutations are also enumerated by Baxter numbers, it follows that PFPs are in size-preserving bijection with mosaic floorplans. This correspondence can be made more precise:

**Proposition 55.** *Every mosaic floorplans (i.e., every equivalence class of floorplans under R) contains exactly one PFP.*

*Proof.* Recall that there are as many mosaic floorplans of size  $n$  as PFPs of size  $n$  (namely,  $Bax_n$ ). Thus, it is enough to prove that every mosaic floorplan contains *at least* one PFP. To prove this statement, we show that every floorplan containing some patterns  $\lrcorner_{\Gamma}$  is *R*-equivalent to a floorplan containing strictly fewer such patterns.

Let  $F$  be a floorplan containing  $\lrcorner_{\Gamma}$ . Consider two tiles  $t_1$  and  $t_2$  forming a pattern  $\lrcorner_{\Gamma}$ , with  $t_1$  located Northwest from  $t_2$ , and such that the distance between the bottom rightmost corner of  $t_1$  and the top leftmost corner of  $t_2$  is minimal among all such patterns in  $F$ . Necessarily, the two segments meeting at the bottom rightmost corner of  $t_1$  form a T-junction, of type  $\perp$  or  $\dashv$ . We assume that it is of type  $\perp$ . The case  $\dashv$  is easily deduced by symmetry (applying reflection along a Northwest-Southeast axis).

To obtain a floorplan  $F'$  *R*-equivalent to  $F$  with fewer patterns  $\lrcorner_{\Gamma}$ , we slide a segment of  $F$ , denoted  $E$ , and defined as follows (see Figure 31(a)).

Il faudrait changer les  $T_i$  en  $t_i$  sur la figure (unification des notations avec la section sur les PFP)

Let  $t_3$  be the tile located immediately to the right of  $t_1$ . By minimality of  $(t_1, t_2)$ , the  $x$ -coordinate of right side of  $t_3$  is strictly larger than the  $x$ -coordinate (denoted  $x_c$ ) of the top leftmost corner  $c$  of  $t_2$ . Now, consider the stack of tiles containing  $t_3$  and all the tiles stacked on  $t_3$  such that

- the  $x$ -coordinates of the left sides of the tiles are weakly increasing from bottom to top and are all smaller than or equal to  $x_c$ ;
- the  $x$ -coordinates of the right sides of the tiles are strictly larger than  $x_c$ .

We consider the tiles of the stack whose left sides have maximal  $x$ -coordinate (denoted  $x_E$ ), and we define  $E$  as the union of all these left sides. We claim that  $E$  is a segment of  $F$ , *i.e.*, that the lower (resp. upper) extremity of  $E$  is a T-junction of the form  $\perp$  (resp.  $\top$ ). This claim is easily proved by contradiction, using the above definition of the stack of tiles, its maximality, and the fact that the T-junction at the bottom rightmost corner of  $t_1$  (which is also the bottom leftmost corner of  $t_3$ ) is of type  $\perp$ . It follows that  $E$  is also the union of the right sides of some (one or several) tiles, and for each of these tiles  $t$ ,  $(t, t_2)$  is a pattern  $\lrcorner$ . The segment  $E$  may be slid to the right until  $x_E > x_c$ , to get a floorplan  $F'$  which is  $R$ -equivalent to  $F$  and contains strictly fewer patterns  $\lrcorner$ .  $\square$

Figure 31(b) shows a floorplan and a PFP that are  $R$ -equivalent.

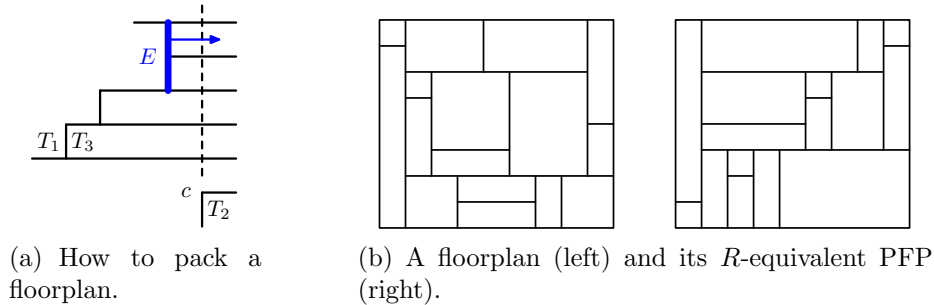


FIGURE 31. Every mosaic floorplan contains exactly one PFP.

### ACKNOWLEDGMENTS

This research has received the support of the ANR, through the ANR – PSYCO project (ANR-11-JS02-001).

### REFERENCES

[1] E. ACKERMAN, G. BAREQUET, R. Y. PINTER, *A bijection between permutations and floorplans, and its applications*, Discrete Applied Mathematics, Vol. 154, Issue 12, 2006, 1674–1684.  
 [2] A. ASINOWSKI, M. BOUSQUET-MÉLOU, G. BAREQUET, T. MANSOUR, R. PINTER *Orders induced by segments in floorplan partitions and (2-14-3,3-41-2)-avoiding permutations*, Electronic Journal of Combinatorics, Vol. 20, No. 2, 2013, paper P35.

- [3] J.-C. AVAL, A. BOUSSICAULT, P. NADEAU, *Tree-like tableaux*, DMTCS Proceedings FPSAC'2011, 63–74 [hal-00618274].
- [4] J.-C. AVAL, A. BOUSSICAULT, M. BOUVEL, M. SILIMBANI, *Combinatorics of non-ambiguous trees*, Advances in Applied Mathematics, Vol. 56, 2014, 78–108.
- [5] G. BAXTER, *On fixed points of the composite of commuting functions*, Proceedings of the American Mathematical Society, Vol. 15, No. 6, 1964, 851–855.
- [6] R. BAXTER, *Dichromatic polynomials and Potts models summed over rooted maps*, Annals of Combinatorics, Vol. 5, 2001, p. 17.
- [7] N. BONICHON, M. BOUSQUET-MÉLOU, E. FUSY, *Baxter permutations and bipolar orientations*, Séminaire Lotharingien de Combinatoire 61A, 2010, Article B61Ah.
- [8] M. BOUSQUET-MÉLOU, A. CLAEISSON, M. DUKES, S. KITAEV,  *$(2 + 2)$ -Free posets, ascent sequences and pattern avoiding permutations*, J. Combin. Theory Ser. A 117 no. 7 (2010) 884-909.
- [9] T. CHOW, H. ERIKSSON, AND C. K. FAN, *Chess tableaux*, Electronic J. Combin. 11(2) (2005), #A3.
- [10] F.R.K. CHUNG, R. GRAHAM, V. HOGGATT, M. KLEIMAN, *The number of Baxter permutations*, Journal of Combinatorial Theory, Series A, 24(3):382–394, 1978.
- [11] R. CORI, S. DULUCQ, G. VIENNOT, *Shuffle of Parenthesis Systems and Baxter Permutations*, J. Combin. Theory Ser. A 43 (1986), 1–22.
- [12] M.-P. DELEST, G. VIENNOT, *Algebraic languages and polyominoes enumeration*, Theoretical Computer Science (vol. 34, 1984), 169–206.
- [13] S. DULUCQ, O. GUIBERT, *Stack words, standard permutations, and Baxter permutations*, Discrete Mathematics, Vol. 157 (1996), 91–106.
- [14] S. DULUCQ, O. GUIBERT, *Baxter permutations*, Discrete Mathematics, 180 (1998), 143–156.
- [15] S. FELSNER, E. FUSY, M. NOY, D. ORDEN, *Bijections for Baxter families and related objects*, Journal of Combinatorial Theory Series A (Vol. 118(3), 2011), 993–1020.
- [16] I.M. GESSEL, G. VIENNOT, *Binomial determinants, paths, and hook length formulae*, Advances in Mathematics 58, 1985, 300–321.
- [17] S. GIRAUDO, *Algebraic and combinatorial structures on Baxter permutations*, FPSAC 2011, Reykjavík, Iceland, DMTCS proc., 2011, 387–398.
- [18] X. HONG, ET AL., *Conner block list: An effective and efficient topological representation of non-slicing floorplan*, In Proceedings of the International Conference on Computer Aided Design (ICCAD '00) 8-12.
- [19] O. GUIBERT, *Combinatoire des permutations à motifs exclus en liaison avec mots, cartes planaires et tableaux de Young*, PhD thesis (Univ. Bordeaux, 1995).
- [20] S. LAW, N. READING, *The Hopf algebra of diagonal rectangulations*, Journal of Combinatorial Theory, Series A, 119, 2012, 788–824.
- [21] B. LINDSTRÖM, *On the vector representation of induced matroids*, Bull. London Math. Soc., 5:85–90, 1973.
- [22] A. POSTNIKOV, *Total positivity, Grassmannians, and networks*, arXiv:math/0609764v1, 2006.
- [23] N. READING, *Lattice congruences, fans and Hopf algebras*, J. Combin. Theory Ser. A 110 (2005) no. 2, 237–273.
- [24] K. SAKANUSHI, Y. KAJITANI, D.P. MEHTA, *The quarter-state-sequence floorplan representation*, IEEE Trans. on Circuits and Systems I: Fundamental Theory and Applications, 50:3 (2003), 376–386.
- [25] N.J.A. SLOANE, *The On-line Encyclopedia of Integer Sequences*, (2007) published electronically at [www.research.att.com/~njas/sequences/](http://www.research.att.com/~njas/sequences/).
- [26] G. VIENNOT, *A bijective proof for the number of Baxter permutations*, Troisième Séminaire Lotharingien de Combinatoire, Le Klebach (1981), 28–29.
- [27] X. VIENNOT, *Alternative tableaux, permutations and partially asymmetric exclusion process*, Slides of a talk at the Isaac Newton Institute in Cambridge, 2008.

- [28] J. WEST, *Generating trees and the Catalan and Schröder numbers*, Discrete Mathematics, vol. 146 (1995), pp. 247–262.
- [29] J. WEST, *Enumeration of Reading's twisted Baxter permutations*, talk presented at *Permutation Patterns 2006*, preprint available at <http://www.cs.otago.ac.nz/staffpriv/mike/PP2006/abs/West.pdf>.
- [30] B. YAO, H. CHEN, C.K. CHENG, R.L. GRAHAM, *Floorplan representations: Complexity and connections*, ACM Transactions on Design Automation of Electronic Systems, 8:1 (2003), 55–80.

(JCA) LABRI - CNRS, UNIVERSITÉ DE BORDEAUX, 351 COURS DE LA LIBÉRATION, 33405 TALENCE, FRANCE.

*E-mail address:* `jean-christophe.aval.1@u-bordeaux.fr`

(AB) LABRI - CNRS, UNIVERSITÉ DE BORDEAUX, 351 COURS DE LA LIBÉRATION, 33405 TALENCE, FRANCE.

*E-mail address:* `boussica@labri.fr`

(MB) INSTITUT FÜR MATHEMATIK, UNIVERSITÄT ZÜRICH, WINTERTHURERSTR. 190, CH-8057 ZÜRICH, SWITZERLAND, AND, UNIVERSITÉ DE LORRAINE, CNRS, INRIA, LORIA, F-54000 NANCY, FRANCE

*E-mail address:* `mathilde.bouvel@loria.fr`

(OG) LABRI - CNRS, UNIVERSITÉ DE BORDEAUX, 351 COURS DE LA LIBÉRATION, 33405 TALENCE, FRANCE.

*E-mail address:* `olivier.guibert@labri.fr`

(MS) LABRI - CNRS, UNIVERSITÉ DE BORDEAUX, 351 COURS DE LA LIBÉRATION, 33405 TALENCE, FRANCE.